Interner Bericht

DLR-IB-FT-BS-2024-101

Simulation of helicopter rotor hub vibration reduction using passive method within a workflow integrated environment

Hochschulschrift

Anil Yasasvi Turumella

Deutsches Zentrum für Luft- und Raumfahrt

Institut für Flugsystemtechnik

Braunschweig

DLR Deutsches Zentrum für Luft- und Raumfahrt
German Aerospace Center

Interner Bericht

DLR-IB-FT-BS-2024-101

Thesis Report

Simulation of helicopter rotor hub vibration reduction using passive method within a workflow integrated environment

Anil Yasasvi, Turumella
Institute of Flight Systems
Braunschweig

9	Seiten
47	Abbildungen
6	Tabellen
41	Literaturstellen

Deutsches Zentrum für Luft- und Raumfahrt e.V.
Institut für Flugsystemtechnik
Abt. Hubschrauber
Lilienthalplatz 7, D-38108 Braunschweig

Braunschweig, 11.06.2024

Institutsleiter:	Prof. Dr.-Ing. Stefan Levedag
Abteilungsleiter:	Dr.-Ing. Klausdieter Pahlke
Betreuer:	Dr.-Ing. Rohin Kumar Majeti
Verfasser:	Anil Yasasvi Turumella

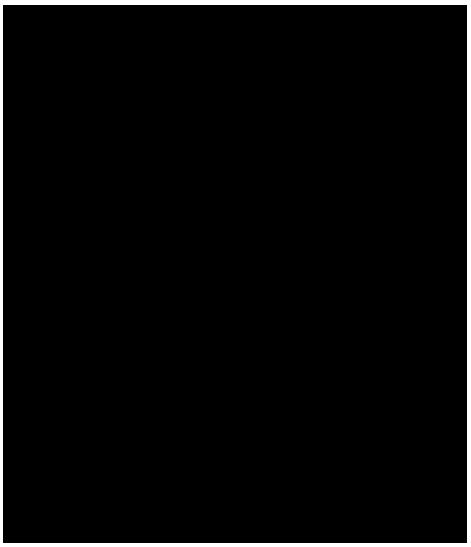

Declaration

I hereby declare that I have written the master thesis report independently without the help of third parties and have written without using other than the specified sources and aids.

All passages taken literally or analogously from the sources used are individually identified. This work has not yet been submitted to any other examination authority and has also not been published.

Acknowledgment

I would like to thank everyone who actively supported me during the preparation of this master's thesis. Prof. Martin Schröck for making it possible and for supervising my master thesis and also the technical department Ernst-Abbe-Hochschule University of Applied Sciences, Jena.

My special thanks go to Dr. Rohin Kumar Majeti, who is my supervisor at the Institute for Helicopter Department at the DLR in Braunschweig, also for being always at my side in numerous technical discussions and provided me with helpful suggestions for the subject of this work.

Special thanks to my parents, friends and family for their support. This is certainly not enough but thanks for supporting me all the time and all the things we have shared.

Abstract

Rotor blade vibration is one of the major hazards for the helicopter affecting the flight's performance. For this purpose, an optimization procedure was developed which involves integrating VAST (Versatile Aerodynamic Simulation Tool) into the workflow-integrated environment RCE (Remote Control Environment) and using a Single-Objective Genetic optimization algorithm as the optimizer.

Initially, to test the optimizer and process of optimization and integration of tools in RCE, an experiment is carried out by integrating Fusion 360 and FreeCAD. The idea behind the integration of Fusion 360 for CAD modelling and FreeCAD for FEA of the CAD model imported from Fusion 360 to perform optimization where the Objective is to retain minimal material which is sufficient to withstand the stresses. The design variables for the optimization process are the diameter of the circular hole, the distance between the center of the coordinate system and the center of the hole towards the X direction, and the distance between the center of the coordinate system and the center of the hole towards the Z direction. To achieve the best parameters and best design variables for the optimization process both Single Objective Genetic Algorithm and Evolutionary Algorithm are used. The best parameters and best objective function are achieved through a Single Objective Algorithm in RCE.

The whole optimization process for minimal rotor blade vibration is performed by carrying out three experiments at the forward flight descent condition by placing three tuning masses whose total weight is the summation of 10% weight of the rotor blade. The experiments carried out for minimizing the objective function are by placing the three tuning masses at varying locations on the elastic axis of the rotor blade, the other experiment when the masses are placed offset to the elastic axis at varying positions, and the last experiment when the masses placed offset to the elastic axis at varying locations with varying twist angle.

The design variables are the three masses, the locations on the rotor blade, the distance offset to the elastic axis, and the twist angle. The resulting best objective function is compared to the objective function with the baseline condition where the masses are not placed on the helicopter rotor. The results from the experiments to achieve the vibration reduction using tuning masses are successful. The objective function has been minimized by 65.37% as compared to the baseline objective function.

Table of Contents

List of Figures

List of Tables

List of Symbols

AI: auto-rotational inertia index

EI_F: blade cross section flap-wise bending stiffness

EI_C: blade cross-section chordwise bending stiffness

GJ: blade cross-section torsional stiffness

H: longitudinal hub force

I_b: blade mass moment of inertia concerning hub

M_{bF}: blade root flap-wise bending moment

M_{bI}: blade root in-plane bending moment

M_T: blade root twisting moment

$M_{X:}$ hub rolling moment

M_Y: hub pitching moment

M_Z: hub yawing moment

N: number of blades

R: blade radius

S_X: blade root radial tension force

S_Y: blade root in-plane shear

S_Z: blade root vertical shear

T: vertical hub force

V_∞: forward flight speed

W: helicopter gross weight

(X, Y, Z): hub reference axes

Y: lateral hub force

c: blade chord length

f_i: i^{th} natural frequency

h: blade box-beam height

k: integer for vibratory hub loads

m: blade cross-section mass per unit length

FEA: Finite Element Analysis

1. Introduction

Helicopter vibration is defined as the oscillatory response of the helicopter airframe to the rotor hub forces and moments [1]. Although there are other vibration sources like engine and transmission, and aerodynamic loads on the fuselage and tail rotor, their effects are mostly local. The major source of vibration is the vibratory hub loads from the main rotor [3]. These loads are transmitted to the fuselage through the rotor hub, and a reduction in these loads is expected to reduce the vibrational level of the whole helicopter. Therefore, in this thesis, vibrations which are induced by main rotor forces and moments were considered.

Helicopter operation has strong aerodynamic and structural dynamics interactions therefore optimization algorithms are also used in the rotorcraft industry so that lighter, safer, cheaper, and high-performance helicopters can be designed. However, while algorithms solve the mathematical relations the physical world should also be represented. Rotorcraft comprehensive analysis is the best choice for this purpose which has been very popular in the rotorcraft industry due to its fast and reliable solutions for the whole helicopter. Therefore, if the coordination between optimization algorithms and rotorcraft comprehensive analysis is ensured, rotorcraft design can benefit from multidisciplinary optimization. For this purpose, an optimization procedure that can reduce the main rotor-induced vibrational level was proposed.

1.1. Rotary Wing vs Fixed Wing

The powered flight is composed of three main functions control, propulsion, and lift. Powered aerial vehicles are classified into fixed-wing and rotary-wing categories according to the way of achieving these functions. The first concept of a powered aircraft was the fixed wing which achieves three main functions with independent subsystems. The lifting force is generated by the wings, propulsion from engines overcomes drag, and control surfaces adjust the attitude of the aircraft. On the other hand, helicopters, or generally rotorcraft, use rotating wings to provide lift, propulsion, and control [1]. The rotor is the responsible component for the main functions and is composed of rotating wings which are named blades. The rotatory wings allow the helicopters to take-off, land and also allows to fly with forward and backward condition.

In a fixed-wing aircraft, the airspeed experienced by the wings is the same speed that the aircraft flies with. A difference in airspeed between wings is only possible in some maneuvers and gust conditions which are usually insignificant. The lift generation depends on the square of the airspeed faced by wings, and then at low airspeeds, the lift force is not enough to overcome gravity. Aircraft speed must be increased by the propulsive force until a satisfactory airflow is reached over airfoils. Therefore, the main disadvantage of separated functions of fixed-wing aircraft is that they require a runway depending on their take-off weight to accelerate to the required airspeed over wings so that the necessary amount of lift can be generated. The same problem also arises in landing such that to maintain the lifting force equal to the aircraft weight, fixed-wing aircraft approach to the ground with a flight speed and can only be slowed down after the landing gears touch down so that the airplane weight is carried by the reactive forces on the landing gears.

Although lift generation with fixed wings is very efficient and fixed-wing aircraft serve many purposes from transportation to fighting, they cannot manage certain missions including vertical take-off and landing, backward flight, low-speed flight, and flight within urban areas. This problem restricts the mission capability of fixed-wing aircraft if there is no suitable runway. Examples of such missions can be given as, rescue from sea or delivery of troops to a mountain [2]. Therefore, the solution is to perform such missions by generating lift at stationary conditions or low flight speeds. The most practical solution to this problem is to rotate the wings so that depending on the angular speed and length of the rotating wings, the aerodynamic surfaces face an airspeed distribution which generates lift without any need to the forward flight speed. That solution provides a great maneuvering capacity to the helicopters at zero, negative, and low flight speeds. In addition to its lift function, the rotor is also used for propulsion and control. It is possible to fly forward by tilting the rotor disc such that a component of rotor thrust supplies enough propulsive force to overcome the drag force. In the same manner, rotor disc tilt can provide moments around the helicopter's center of gravity so that lateral and backward motions and other maneuvers such as pull-out and roll-over can be performed. As being the main source of flight, the understanding of the rotor and

its operational environment which will be discussed in Section 1.2 is essential in understanding the dynamic and vibratory behavior of the Helicopters.

1.2. The Rotor and its Operational Environment

As previously mentioned, the rotor is the main source of lift, propulsion, and control in helicopters. The rotor blades rotate at high speeds in a complex unsteady aerodynamic environment and the interaction of blades with this aerodynamic environment is the main source of vibration [2]. Before going into the details of the vibration problem, the rotor with its main components should be discussed so that the reasons for vibration and its solution can be clearly understood. The major characteristic of a helicopter is its vertical flight capacity which defines the size of the rotor. It is observed that the blades of helicopters are long slender structures and most of the time rotor diameter is comparable to the fuselage length. Because of its size, the rotor is the most dominant component of the helicopter in all aspects including aerodynamics, dynamics, structural dynamics, strength, stability, cost, and maintenance of the whole aircraft.

The reason for the large diameter comes from the disc loading which is the ratio of the thrust to the rotor disc area. For a rotary wing aircraft, to overcome gravity forces, the rotor thrust is obtained by accelerating the air downwards which causes induced power loss. The cost of vertical flight capacity is proportional to the square root of loading of the rotor disc.

Therefore, increase in the rotor diameter causes reduction in disc loading for a given gross weight and reduces the induced power loss which in turn increases the vertical flight capacity. There are also other structures with rotating wings like airplane propellers but since they operate in high-speed axial flow and at a lower thrust level as compared to body weight, their effects are local and their size is very small as compared to that of the helicopter rotor [1].

The outer part of the rotor is composed of the aerodynamic surfaces which are called rotor blades. On any aircraft, whether it is fixed wing or rotary wing, aerodynamic surfaces generate the forces and moments to overcome the resisting force and moments. For the helicopter flight, rotating blades which are of slender and elastic structures assists the necessary forces and moments. Figure 1 represents a simplified geometry of blade planform and cross-section.

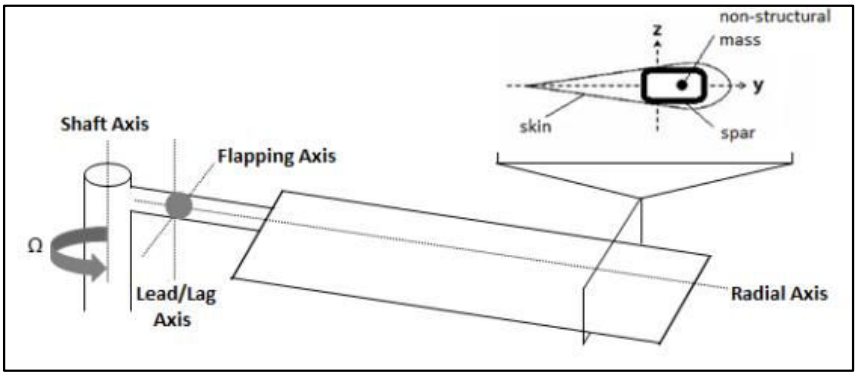

Figure 1. A Typical Rotor Blade and its cross-section

A rotor blade has a free boundary condition at its tip and is connected to the rotor hub at its root. Relative motion at the rotor hub is allowed by hinges or elastic supports depending on the root design and they are called fundamental blade motions. The blade motion which is perpendicular to the rotor plane is called out-of-plane or flapping motion whereas the motion which occurs in the rotor plane is called in-plane or lead-lag motion. The third motion is the rotation around a radial axis called feathering or pitching. In addition to the fundamental motions governed by the root connections and pitch bearing, there are also elastic motions of the blades because of the blade elasticity. The elastic motion that bends the blade out of the rotor plane is named out-plane bending or elastic flapping. Similarly, the bending motion occurring in the rotor plane is the in-plane bending or elastic lead-lag. Additionally, the deformation around the radial axis is called twisting. Axial elongation along the radial axis and cross-section warping can also be included but their effects are limited to some special cases [3]. The aerodynamic and inertial loads occur due to the fundamental and elastic blade motions.

Drag, lift, and pitching loads originate from rotor aerodynamics. From the nature of the rotor, rotation causes a centrifugal force on the blade which has an important stiffening effect due to high speeds of rotation. Another effect of the rotation is the gyroscopic loads when the rotation axis tilts. The most significant one is the in-plane Coriolis load due to the flapping. When blades flap, the blade center of gravity moves in the radial direction, and due to conservation of momentum principle acceleration or deceleration occurs in the rotor plane [2]. Furthermore, there are other sources of coupling due to rotation field, blade external geometry, and blade internal geometry.

The representative cross-section of the rotor blade in Figure 1 is composed of spar, skin, and non-structural mass. The shape of the skin defines the airfoil shape. The maximum lift coefficient (CL_{max}) defines the rotor solidity and the thrust level. Drag divergence Mach number (MD) should be high enough for low drag at higher forward flight speed and low noise. A high lift-to-drag ratio over a wide range of Mach numbers is required for low power consumption and low autorotation rate of descent. Finally, to minimize vibrations around a radial axis, twisting moments, and prevent high control moments at the blade root a large moment coefficient (C_m) is to be prevented [4].

In this particular representative airfoil, the load-carrying component is the spar of the cross-section. Its distribution over the cross-section and the material properties determines the inertial and stiffness properties of the cross-section. These properties have primary importance in the blade's static and dynamic behavior. Other components which contribute to the stiffness and mass of blade which are erosion shield, honeycomb filler, and other functional parts have their effects on load resistance which are of secondary importance.

From a structural dynamics point of view, rotor blades can be analyzed in one dimension for most of the loading conditions. In other words, the blade's elastic characteristics can be described as functions of radial coordinates. Therefore, elastic properties are evaluated by considering the distribution of the blade structure over the cross section at the relevant radial coordinate [3]. When engineering beam theory is applied, the stiffness resisting out--of-plane and in-plane bending motions are called flap-wise bending stiffness (EIF) and chordwise bending stiffness (EIC) respectively, and twisting deformation is resisted by torsional rigidity (GJ). The flap-wise bending stiffness is calculated around the horizontal principal axis (y-axis of Figure 1), chordwise bending stiffness is evaluated around a vertical principal axis (z-axis of Figure 1) and around the blade radial axis torsional rigidity gets evaluated.

The cross-section mass can be evaluated by the contributions from structural load-carrying elements and non-structural masses. The blade's stiffness can be neglected compared with the blade spar. A typical rotor hub is represented in Figure 2[5].

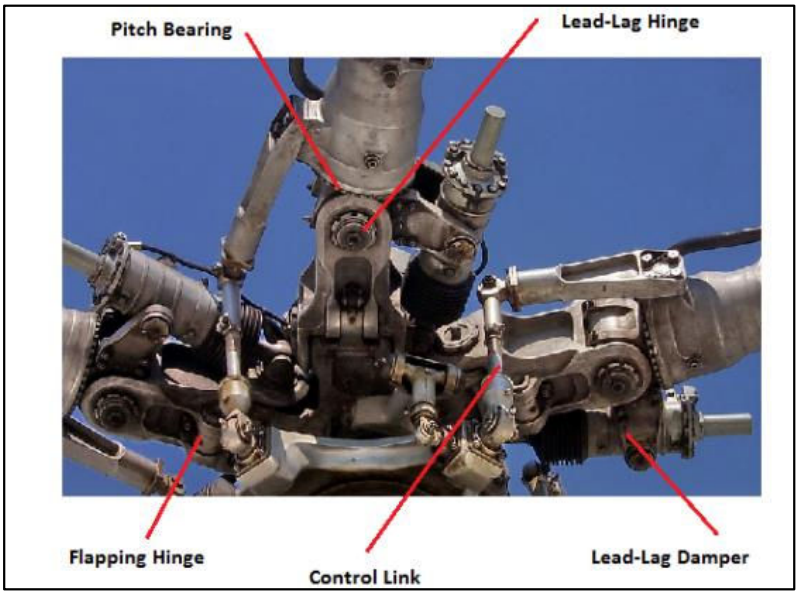

Figure 2. Mi-17 Articulated Main Rotor Hub [5]

Inertial and aerodynamic loads acting on the blades are summed at the rotor hub and transferred to the transmission and fuselage. Control links transfer the pilot control inputs to each blade. Lead-lag dampers prevent the possible unstable motion of blades in the rotor plane. As previously explained pitch bearing allows blade feathering and blade's fundamental motions of flapping and lead-lag are allowed by hinges or elastic root connections. Blades are classified according to type of the connection since each of them has unique dynamic characters. Rotors with hinged connections are called articulated blades. If there is only one flapping hinge passing through the shaft, then this configuration is called teetering. Another type which is named hinge-less blades eliminates the hinges and uses elastic connections to sustain flapping and lead-lag motions. A special variation of the hinge-less blade is the bearing-less blade which also eliminates pitch bearing in addition to the flapping and lead-lag hinges [6].

The control system is required to govern the aerodynamic loads acting on the blade so that lift, propulsion, and control of the helicopter can be managed. These forces depend on the angle of attack and airflow speed faced by the blades. The blade angle of attack is determined by the blade pitch which is also called feathering. A simple blade control system can be seen in Figure 3.

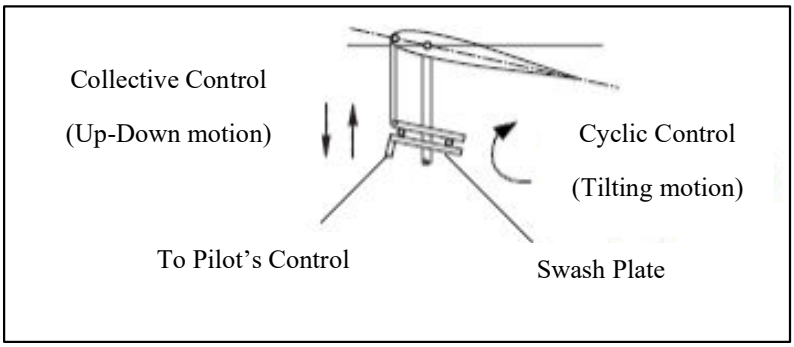

Figure 3. Function of Swash Plate

There are two options in pitch control which are collective and cyclic controls and they are applied by a swash plate which is linked to pilot controls. This plate is composed of two sections which are connected. The lower plate is stationary and linked to pilot controls whereas the upper swash plate is rotating and connected to the blades via control links. When the collective lever is moved, then the swash plate changes its position up or down and all the blades face the same angle change of attack irrespective of their position on the rotor disc. This vertical motion of the swash plate changes thrust output. The other one, cyclic pitch control is used to tilt the rotor disc. Input from the pilot tilts the swash plate in longitudinal and lateral directions. The tilt of the swash plate generates a cyclic variation of the angle of attack over the rotor disc and the thrust vector can be oriented to provide propulsion for forward or lateral flight or moment to the aircraft center of gravity for the maneuvers.

In addition to complexities arising from blade elastic motion and control systems, helicopters also operate in a complex aerodynamic field due to forward flight. Once the rotor is tilted, the longitudinal component of rotor thrust accelerates the helicopter. However, forward flight introduces another problem which is the asymmetric distribution of velocity over the rotor disc which can be seen in Figure 4.

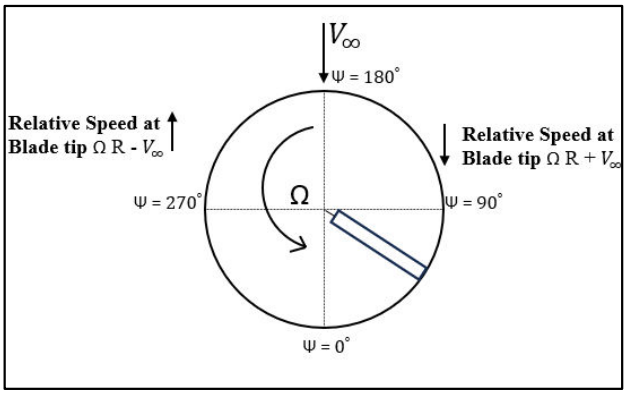

Figure 4. A Counter-Clockwise Rotor in Forward Flight

For a counterclockwise rotor seen from above, the right-hand side faces forward flight speed from the blade's leading edge and is called the advancing side whereas the left-hand side faces forward flight speed from the trailing edge and is called the retreating side. When the angular velocity and forward flight velocity are summed the airspeed distribution in the advancing side is greater in magnitude than that of the retreating side. The differential relative speed distribution on aerodynamic surfaces causes the aerodynamic load on two sides to differ and generate a rolling moment on the body and a large bending moment at the root. This in turn causes oscillatory loads on the blades.

Moreover, to the load asymmetry the aerodynamic environment is more complicated. On the advancing side, the compressibility effects increase as the forward flight speed increases. Another issue to be considered is retreating the side blade stall. As forward flight speed increases the blades at the retreating side face with lower speed and this reduction must be compensated by an increase in the blade angle of attack and then blades start stalling which is the major limit for maximum speed [7]. The final one is the inverse flow region, the blade faces the airflow from the leading edge and this area is measured by the circle having the diameter of the advance ratio μ [8]. Blade-blade, main rotor-tail rotor, and blade-fuselage interactions are also remarkable [9]. The complex aerodynamic operation of the rotor can be seen in Figure 5.

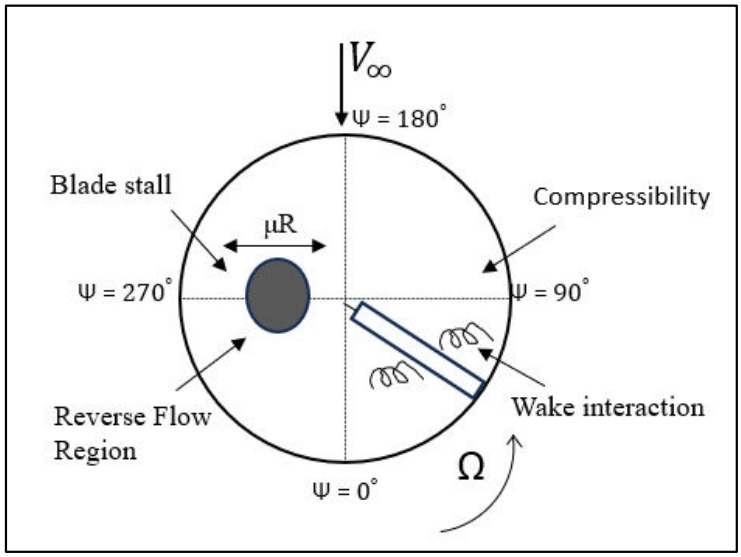

Figure 5. Forward Flight Aerodynamic Environment for a Counter-Clockwise Rotor

Since airflow speed, angle of attack, stall effect, reverse flow, and compressible flow are uniformly distributed over the rotor disc in case of hover flight condition and non-uniformly distributed for other flight conditions, the aerodynamic loads and blade motion resulting from all the rotational, dynamic, and aerodynamic effects are all oscillatory. The oscillations in the load and blade motion are the major sources of helicopter vibration [1].

Although the loads and motion are oscillatory, the periodicity of the rotor simplifies the analyses. In a level flight, the orientation of the helicopter body and the rotor rotation axis remain the same but the rotor still rotates and the time-dependent loads and motion still exist on the rotor. In that case, after transient effects die out the blades face the same loads and motion, if blades pass towards the same azimuthal coordinate (Ψ). In other words, there are variations in loads and motion within the rotor disc however the variations repeat itself at each revolution. Therefore, excluding maneuvers in which there are translational and angular accelerations, the rotor operation is periodic [1]. Using the periodic nature of the rotor, the time domain rotor analysis can be reduced to the frequency domain with the period of 2π and the fundamental frequency of rotor angular speed (Ω). The analysis of the frequency domain can be calculated using the Fourier Series where the variables are time-dependent and represented with mean component and an infinite sum of harmonics which are also the sinusoidal functions of rotor azimuth coordinate at the integral multiples of fundamental rotor frequency. For a general load variable (L) and a general motion variable (X), time-dependent equations can be represented in the frequency domain as [1];

$$L(\Psi) = L_0 + \sum_{n=1}^{\infty}\left[L_{n,c}\cos(n\Psi) + L_{n,S}\sin(n\Psi)\right] \quad 1$$

$$X(\Psi) = X_0 + \sum_{n=1}^{\infty}\left[X_{n,c}\cos(n\Psi) + X_{n,S}\sin(n\Psi)\right] \quad 2$$

Where;

n	: Harmonic Number, n = 1, 2,…	Ψ	: Rotor azimuth angle
L_0	: Steady Load Amplitude	X_0	: Steady Motion Amplitude
$L_{n,c}$	: n^{th} cosine Load amplitude	$L_{n,S}$	: n^{th} sine Load amplitude
$X_{n,c}$	: n^{th} cosine Motion amplitude	$X_{n,S}$	: n^{th} sine Motion amplitude

In equations 1 and 2, the time-dependent periodic variables (L and X) were represented in the frequency domain with the amplitude of each harmonic. For a periodic system, the sum of all the harmonics and the steady value is exactly equal to the time-dependent variable if an infinite number of harmonics is used. Luckily, the amplitudes of higher harmonics are usually negligible and a finite number of terms are sufficient for an accurate representation which should be determined according to the complexity of the problem. The Fourier Series representation is very commonly used in the rotorcraft industry and simplifies the rotor analysis in understanding and solving the equations of motion since the contribution from each harmonic can be analyzed separately and the overall result can be obtained by summing all the harmonics in the range of interest [1].

The dynamics of the rotor are quite complex due to high angular rotation speed, slender elastic blades, and unsteady aerodynamic environment. An understanding of the rotor and its operation is critical in understanding the helicopter vibration and solutions for vibration reduction. Although helicopter vibration requires a lot more knowledge of the rotor and fuselage, the background given in this section provides the necessary background to understanding the major source of helicopter vibrations which is the main rotor oscillatory loads and motion.

1.3. Rotorcraft Comprehensive Analysis

The rotorcraft analysis exhibits difficulties because of the dominance of the main rotor and complex operation environment including high levels of dynamic, structural, and aerodynamic interactions. Due to this complex behavior of rotorcraft, it is essential to design the rotorcraft by using a single code that is capable of simulating this sophisticated flight environment with reliable accuracy and short computation times [35]. This type of analysis is called comprehensive analysis and is widely used in rotorcraft industry. They are specifically written for rotorcraft analysis purposes. To be named as comprehensive, a tool should have the following capabilities:

- Aerodynamics of the rotor, inflow modeling, wake modelling
- Structural dynamic modeling of the blade, natural frequency calculation, blade response to aerodynamic loads
- Trim model of rotor and fuselage
- Evaluation of static and dynamic loads
- Solution of the equations of motion
- Fast Computation

1.4. Induced velocity/Inflow & Dynamic inflow model

When the rotor rotates, the air mass above the rotor is sucked through the rotor disc. This induces a flow perpendicular to the rotor disc, reducing effective angle of attack of the blade section as shown in Figure 6. The induced velocity depends on the blade loading at each section. Since the blade loading varies along radial and azimuthal direction and also with respect to time, the induced velocity is a function of radial distance, azimuth angle and time. And hence, the angle of attack of the airfoil section also varies with respect to radial and azimuthal location. So, the proper estimation of the induced velocities through the rotor disc is very critical in rotorcraft aeromechanical studies.

Currently, there are a range of inflow models starting from very simple uniform inflow model to very complex computational fluid dynamics models. Most of the inflow models are extension of propeller theories like momentum theory and vortex theory. The following inflow models are commonly used in the helicopter flight mechanics simulation tools. They are uniform inflow, Glauert inflow, Drees inflow, Pitt-Peters three state dynamic inflow, generalized dynamic wake model, Wake distortion model, Free wake and Prescribed wake model.

Each inflow model has its own advantages and disadvantages. In general, these inflow models can be categorized into static or time averaged inflow models and dynamic inflow models.

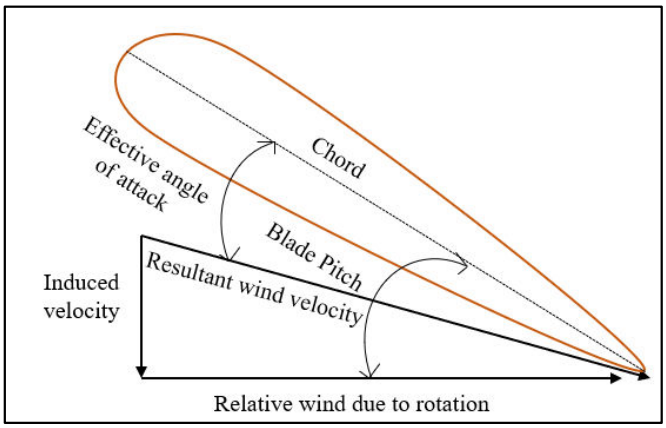

Figure 6. Velocity components and angle of attack at the blade element

For high frequency operations, the static inflow models are inadequate. In general, induced velocity builds up with a time lag to the change in disc loading because the large amount of airmass associated with the rotor needs to be accelerated. And hence there is a need for dynamic inflow models. There are various dynamic inflow models with varying complexities, starting from simple finite state dynamic inflow models to more comprehensive infinite state inflow models.

1.5. The Vibration Problem of Helicopters

The differences in the operational capacities between the fixed-wing and rotary-wing aircraft were introduced in Section 1.1. However, in addition to the operational capacities there are more distinctive features. One of the most significant distinctive features is the vibrational level due to the complex operation of the rotor. The significance of the helicopter vibration problem can be outlined by comparing the vibration-induced problems of fixed-wing and rotary wings. Such a comparison of the failure rates of the hydraulic equipment is presented in Figure 7[10].

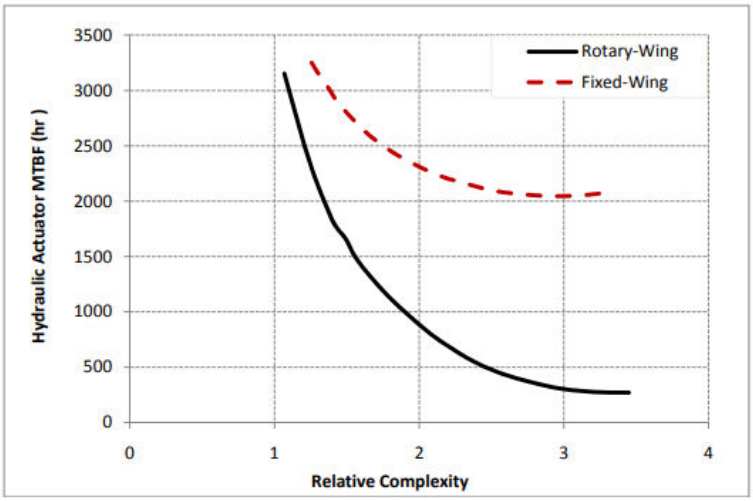

Figure 7. Plot of Fixed-Wing Reliability Vs Rotary-Wing Reliability (Hydraulic Equipment) [10]

The horizontal axis of Figure 7 represents the relative complexity of the hydraulic equipment whereas the vertical axes represent the mean time between failures. For both fixed-wing and rotary-wing equipment with the increase of complexity the mean time between the failure decreases. This reduction is mainly due to the higher vibration levels in rotary-wing aircraft as compared to fixed-wing aircraft.

In rotorcraft performance vibration plays a critical factor. Maximum flight speed is determined by the available power in fixed wing applications and more powerful engine installation usually results in a higher maximum speed. But in rotorcraft power available is not the only limiting factor. As flight speed increases, retreating side blade stall and advancing side compressibility effects induce high levels of vibrations and loads. Because of this reason the design cruise speeds of conventional main rotor tail rotor helicopters usually vary between 150 and 200 knots for modern helicopters [1].

Furthermore, maximum flight speed is not the only performance parameter that is degraded because of vibration. Performance at other flight conditions at which the rotor operates at its wake such as landing, rolling, or autorotation can also suffer from vibrations. More severe vibration levels than those considered do not only decrease performance but also impair flight safety.

Fatigue of the airframe, the rotor blades, and other components is another significant result of the helicopter vibrations. The rotor vibratory loads at the integral multiples of the rotor speed frequencies are the important source of the airframe fatigue loading [11]. The rotor blade operates under an oscillatory aerodynamic environment which was early mentioned in Section 1.2. Under these loads the blade response is quite complex which also includes coupled in-plane and out-of-plane bending, axial elongation, and twisting deformations. More or less all the sections of the blade encounter these oscillatory elongations therefore the whole blade should be evaluated for fatigue. In addition to the airframe and blades, the flight equipment also suffers from fatigue loading [11].

Last but not least, the vibration effect on the flight crew and passengers should not be underestimated. A high level of vibration causes whole-body vibration which occurs when the human body is supported by a surface that is shaking. The vibration from the shaking surface is transmitted through the body of the human in contact with the surface including the skeleton, nervous system, and spine [12]. In general, this whole-body vibration reduces flight comfort. Furthermore, the effects are more severe in the long term. Especially, back pain is a common complaint for helicopter crew which is mostly related to the whole-body vibration [13]. The vibrations cause the stressing of intervertebral discs and paravertebral muscles which serve as the absorber system of the spine [14]. In addition to comfort and health, pilot vision may be blurred and there are cases where pilots are unable to read the flight instruments which is a significant safety problem [2]. At each design phase, possible vibration sources should be handled carefully.

1.6. Helicopter Vibration Reduction

The discussions on the vibration problem of the helicopters and possible consequences in Section 1.3 prove that, the rotor induced vibrations affect the whole body, crew, and payload significantly. Because of these problems, vibration reduction and control are important in order to improve flight safety, passenger comfort, equipment reliability, and material life of components [8]. Therefore, the vibration reduction techniques should be clearly understood and implemented into design to achieve safe and competitive designs.

1.7. Vibration Reduction Techniques

The benefits of vibration reduction in rotorcraft which were discussed in Section 1.4 have led the designers to work on the vibration reduction techniques which achieve vibration reduction by reducing the amplitude and/or alleviating the excitation loads. The techniques can be passive or controlled actively. The passive techniques do not require any actuation and try to reduce vibrations after the vibratory loads are generated. Also, active method acts according to the calculated vibration on the helicopter and tries reduce vibratory loads by producing opposing air-loads [15].

The active and passive vibration reduction techniques are effective in controlling the vibrations that exist for a completed design. However, the main source of the rotor-induced vibrations is due to the aeroelastic behavior of the rotor which plays a key role in the helicopter design. If the design and modification for reduced vibration level are systematically included in the design or modification phase, the level of vibrations can be reduced at the source.

a) Passive Vibration Reduction Techniques

Passive vibration reduction can be achieved by self-actuated systems which include vibration isolation, absorption, and attenuation. The isolators reduce the undesirable effects of vibration by designing the connection between the body which is required to be isolated and the foundation which is the source of vibration itself [16]. On helicopters, their location is in between the critical equipment on the fuselage and the supporting structure that transmits the vibration. They are spring mass damper systems and their working principle is represented in Figure 8.

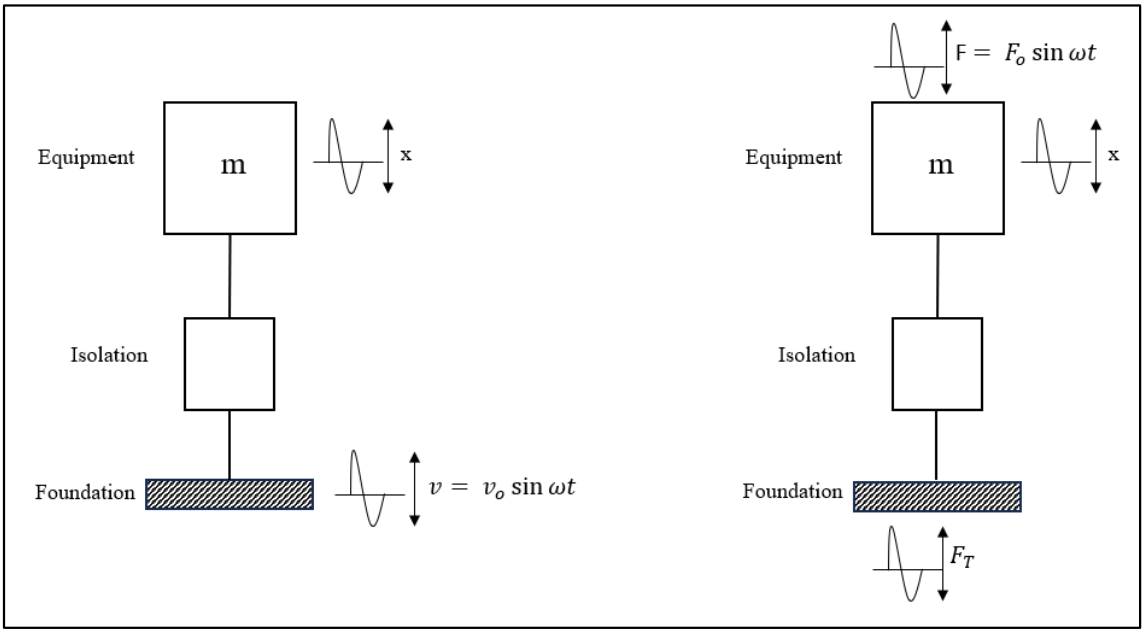

Figure 8. Schematic Diagrams of Vibration Isolation Systems: (A)Vibration Isolation from a Vibrating Foundation; (B) Vibration Isolation from a Vibratory Excitation Force

According to the Figure 8 the isolators either reduce the magnitude of the vibratory motion transmitted from the vibrating foundation (A) or reduce the magnitude of force transmitted from the foundation (B). The pilot seat, avionics and cockpit instruments can be counted among the critical equipment on a helicopter on which isolators are commonly applied [3]. The foundation of a helicopter is the airframe structure mainly excited by the vibratory loads coming from the main rotor.

Vibration absorption refers to extra degrees of freedom addition so that the unwanted effects of vibration are transferred to new degree of freedom rather than to the structure [16]. The well-known absorbers in helicopters are bifilar absorbers and pendulum absorbers, these absorbers can be mounted on the blade in flap wise and in-plane directions.

The attenuators are the non-structural masses which are added to the rotor blade which help in moving blade natural frequencies away from excitation frequencies. They are usually applied at blade tip or mid-span [17]. All three types of the passive vibration reduction techniques are effective at a specific tuning frequency at which the vibratory loads are supposed to be reduced. If vibratory loads exist at any other frequency, the techniques are ineffective and additional vibration reduction systems should be implemented.

b) Active Vibration Reduction Techniques

The active vibration reduction systems are also called excitation reducers which generate opposing aerodynamic loads so that the vibratory loads are cancelled [17]. The most popular active control systems are the higher harmonic control, active flaps and smart structure application on rotor blades.

The swash plate control excites the surrounding air once in every rotor revolution in normal operation as it was discussed in Section 1.2. The idea behind the higher harmonic control (HHC) is to excite the swash plate at a higher frequency in addition to the 1/rev cyclic input so that the cancellation of vibratory air loads occurs due to additional excitation that cancels the vibratory air loads [18]. A sample system is presented in Figure 9[18].

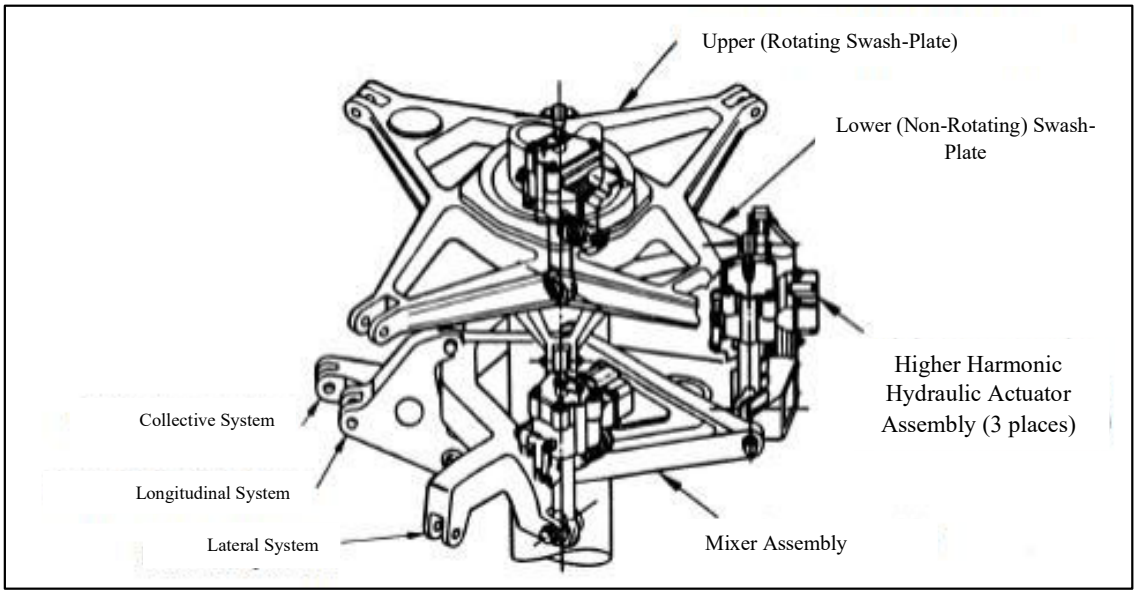

Figure 9. Higher Harmonic Application [18]

The system in Figure 9 is a sample HHC application to a helicopter having 4 blades in order to reduce vibrations at the blade passing frequency. The system measures the vibrations by using the accelerometers located at the pilot seat. The measured vibrations which are supposed to be reduced are converted into signals and then fed into the flight computer. The flight computer calculates the necessary motion of the swash plate. The appropriate combination of the vertical and tilting motions of the stationary swash plate creates the required cancelling loads [18]. Since the cancelling loads reduce vibratory loads, which are the sources of the transmitted vibrations to the fuselage, the vibrations on the pilot seat can also be reduced.

Individual blade control (IBC) is an improved method of HHC. Here, each blade's pitch is excited and better results can be obtained with the addition of multiple control degrees of freedom [19]. There are also other ways of exciting blade individually which is the active flap control [20] and smart blade [21]. The flaps located on the rotor blades are actuated such that the resulting air loads cancel the vibratory loads as in the case of HHC. There is an increase in the number of flaps per blade. This method consumes less power than IBC with a mechanically simpler system [20]. Smart blade concepts make use of piezoelectric actuators. Depending on the level of vibrations, the elastic twist of the blade is altered by using the actuators and therefore the vibratory loads can be reduced [21].

1.8. Design and Modification for Reduced Vibration Level

Since the solutions of passive and active vibration reduction systems have the aim of reducing response or loads for a given system, they can be considered as external applications. Depending on the application the external systems introduce extra weight and drag which degrade performance. Furthermore, the effectiveness of the external applications strongly depends on the vibrational level of the clean structure and its application required to be performed after carrying out costly flight tests.

In addition to performance and cost drawbacks, the local isolation of vibrations solves the problem at the point of application, and then the remaining body may still face significant level of vibrations. Therefore, the vibration levels should be carefully considered at the design or modification stages of a rotorcraft so that the vibrations could be reduced before the product is finalized [2].

The design and modification of helicopter structures can be performed depending on the sources of the vibration [22]. The main sources are aerodynamic blade loading, blade dynamic response as it was described in Section 1.2 and fuselage response to the loads transferred through the rotor hub. Therefore, a reduced vibration level in helicopters can be achieved by smooth aerodynamic loading, favorable blade dynamics and controlling the response of the fuselage.

The aerodynamic design of the blades has strong contribution on the vibratory loads. Periodic loading in forward flight, compressibility and stall effects and the aerodynamic interaction between blades are responsible for the oscillatory aerodynamic loading. The activities aim to reduce the undesirable effects of these sources. Blade tip geometry can be designed to prevent advancing side shocks, blade twist can be distributed to reduce the retreating side stall loading. The wake of the blades should be considered in order to reduce the level of interference between blades. Furthermore, the number of blades has also important effect on the interference of the blades [22].

The other source of vibration which originates from rotor blades is the blade dynamic response. The undesirable effects of blade vibration are the fatigue loading on the blade and the vibratory load amplification on the rotor hub which is transferred to the fuselage. The favorable blade response can be achieved by proper mass and stiffness distribution of the blade. At the same time blade natural frequencies should also be separated from aerodynamic excitation frequencies so that resonant operation is avoided [22].

The vibratory loads from the rotor origin are transferred to the fuselage. As the fuselage responses to these loads, the dynamic response is significant in terms of the vibration levels acting on the structure, cockpit, crew, equipment and payload. The solution is to adjust the fuselage natural frequencies, so that any resonance with the vibrations from the rotor hub reduces. This can also reduce the level of interference between the rotor and the fuselage [22].

Whatever the source of vibration and its solution are, design and modification for reduced vibrational level involves complex engineering work. The rotor system and operation are very complex and a large number of variables have significant impact on the helicopter vibration.

Furthermore, a low vibration design does not necessarily mean that the design is feasible because of the side effects. Therefore, the problem can be stated as to reduce the vibrational level of the helicopter as much as possible within a design space which includes a large number of variables and constraints. Optimization algorithms provide effective solutions for such problems when they are coordinated with rotorcraft analysis tools. For this reason, the design and modification activities for reduced vibrational level should be handled as an optimization process and that process is composed of objective function, constraints and design variables.

The role of comprehensive model in this process is to provide the values of the objective function and constraints for the assigned design variables, where the objective function is defined as the model output to be minimized, constraints are selected in order to prevent unrealistic results and design variables are the proper model inputs which are sensitive to the optimization problem.

1.9. Articulated Blade

Blade articulation is necessary to relieve the bending moment at the root of the blade in forward flight [1]. An articulated blade which was first introduced by Juan de la Cierva in 1920s provides a simple and an effective solution to this problem so that it makes the forward flight possible. The idea was to let the blade move up and down freely, so that the bending moments at the blade root can be eliminated which in turn prevents the transfer of rolling moment to the fuselage. Figure 10[8] provides a typical articulated blade-hub connection [8].

The hinges allow the blade to move in flap-wise and lag-wise directions. The other relative motion is provided by the feathering bearing around which blade pitching motion is performed. In addition to the hinges, a damper in lead-lag direction is always added to the blade root in order to damp Coriolis forces and prevent ground resonance instability [1].

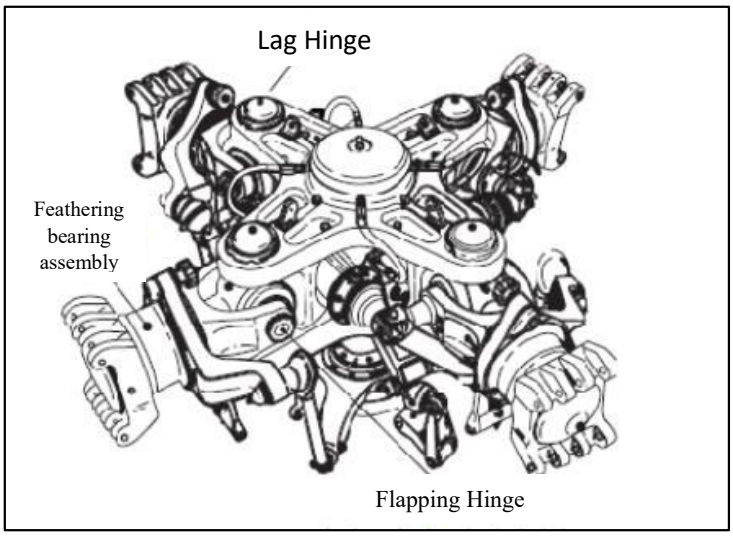

Figure 10. Typical Articulated Blade [8]

Although the relief of moments at root prevents rolling motion of rotor; the bending moment cannot be transferred to the fuselage because of hinged boundary condition and this in turn decreases the maneuvering capacity. In this case, the maneuvering loads can only be achieved by increasing thrust and/or tilting rotor disc via cyclic input. The complexity due to hinges and dampers is another disadvantage of the articulated blade assembly. Maintenance costs of the Hinges increases significantly as the hinges operate under high centrifugal loads whereas high parasite drag is generated at bulky rotor hub. It is comparable with the drag output of rest of the helicopter [36].

1.10. Hingeless Blade

In the previous section, an articulated blade was investigated and the disadvantages of mechanical complexity and loss of control power of these rotors were briefly discussed. In order to reduce maintenance and manufacturing costs and achieve an aerodynamically clear configuration with higher control power, hinges are replaced by flexible elements. Many modern designs have made use of this concept and Westland Lynx and Bo105 were the first two produced hinge less helicopters [37]. Figure 11[8] illustrates a typical hinge less blade-hub connection [8].

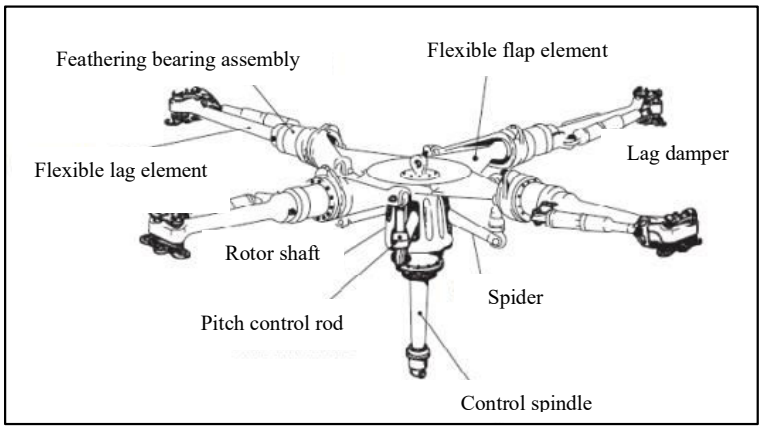

Figure 11. Typical Hinge less Blade [8]

The flexible elements perform the same function of hinges but this time flap wise and edgewise bending moments are generated at the blade root. The maneuvering capability of the helicopter is increased by the flapwise bending moment, as the extra maneuvering load component in addition to the rotor thrust tilt exist. However, these flexible elements should be designed such that the moments at the blade root does not cause rolling of the fuselage and the root stresses remain under critical levels. Furthermore, as in the case of articulated blade, there is still a necessity of lead-lag damper for stability issues and a feathering bearing for blade pitching motion. Although rare yet, some designs also try to eliminate feathering bearing by torsional flexible elements [38].

1.11. Literature Survey

The studies on the analysis and design of helicopter rotor blades for reduced vibration level by using optimization techniques have become popular after comprehensive analysis gained acceptance in rotorcraft industry. This section outlines the studies in the rotor blade optimization for reduced vibration levels and aims to provide a chronological history.

Through [39] the authors optimized non-structural tuning masses to minimize vertical shear forces. They analytically optimized the locations and mass values of multiple tuning masses (Figure 12). Using CAMRAD/JA the optimization procedure was performed to reduce the harmonics of hub-shear for a four bladed rotor, where the design variables are the tuning masses and mass locations on the rotor blade. The tests were performed by placing 3 tuning masses and 6 tuning masses on the rotor blade in the forward flight condition, and obtained the results explaining more tuning masses on the rotor blade decrease the blade vibration.

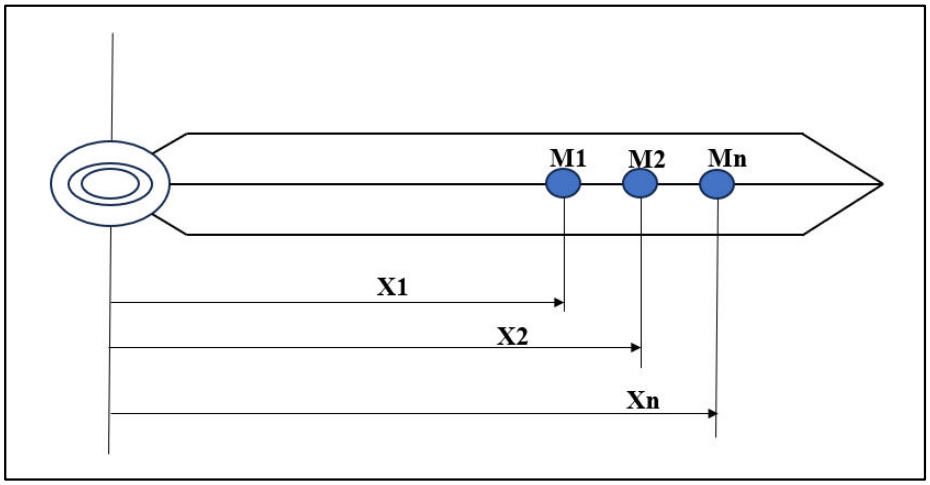

Figure 12. Design variables of masses placed at multiple locations on the helicopter rotor blade

A thesis on the optimal design of helicopter rotor blades for optimum dynamic characteristics was published by Ko in 1985 [23]. In that articulated rotor blades were optimized for the objective of natural frequency separation and weight reduction by using CONMIN gradient based optimization algorithm. Finite element formulation was used in evaluating the natural frequencies of the blades. The cross-section wall thickness and nonstructural masses were defined as the design variables. Constraints on the stress, size of nonstructural mass and the thickness of the beam were used.

Friedman and Celi conducted a study on the structural optimization of rotor blades with swept tips subject to aeroelastic constraints [24]. The objective function was the vibratory rotor hub shear forces of an isolated rotor which are transmitted to the fuselage. The interaction of the blade natural frequencies with aerodynamic excitation frequencies was limited. An aeroelastic code consisting of a finite element formulation with trimming capacity calculations of the hub loads and CONMIN optimization algorithm performed for the optimization task. Here, the cross-section wall thickness and width were the design variables for single cell and double cell beams.

The strategy for the combined structural, inertial, dynamic, aeroelastic, and aerodynamic performance characteristics was discussed by Peters and Cheng [25]. The gradients were provided analytically by a finite element code to optimization algorithm CONMIN. The blade natural frequencies were formulated as the objective function. Two methods were tried in defining the design variables. First one was using cross section dimensions and evaluating cross section inertial and stiffness values from the dimension which had constraints on the dimensions. The second one was directly using the inertial and stiffness distributions and then post-processing for the blade cross section dimensions for the optimum blade which had constraints on the stiffness and inertial quantities. Both methods were successful in the analysis. Furthermore, the stress constraint was not found to be important when only natural frequencies were considered and no section reached yield stress. However, when the blade fatigue life was included in the analysis, the stress constraint became a critical factor.

Lee implemented genetic algorithm to rotorcraft multidisciplinary optimization in 1995 [26]. The purpose of using genetic algorithms is their applicability to parallel computing which is a big advantage in multidisciplinary optimization so that the multidisciplinary problems can be handled by dividing the whole system into subsystems. A finite element based multibody formulation was used to model the blade. A weighted sum of vertical vibratory hub loads was formulated as the objective function which was subjected to the design constraints including power required, autorotational inertia, natural frequencies, rotor thrust, blade weight and buckling stress. The design variables were the tuning masses, blade cross section dimensions, and its initiation point, rotor RPM, and the ply angles of the cross sections.

By using response surface approximation, the objective function was represented as second order polynomial function of design variables. Ganguli used response surface approximation, for optimizing the rotor blades for reduction in vibratory hub loads in 2002 [27]. Design variables were blade flap wise and chordwise bending stiffnesses and torsional stiffness. The optimization was implemented on a hinge less blade with uniform properties. In 2006, Bhadra and Ganguli improved this study by including free wake modeling [28]. In 2008 Murugan et al followed the similar procedure with a robust optimization so that the uncertainties in the design variables were considered [29]. Glaz et al used multiple surrogates together with neural networks in blade vibration reduction in 2009 [30].

In 2004, Viswa Murthy and Ganguli optimized the deflection harmonics of the blade multiple trailing edge flaps for the reduction in vibratory hub loads by putting constraints on the deflection of flaps [31]. The University of Maryland Rotorcraft Analysis code was coupled with a gradient based optimization algorithm.

Stacey, Harrison, and Hansford published a journal in 2008 which is based on the advances in British Experimental Rotor Program that also includes optimization of rotor blade to reduce vibration levels [33]. An inhouse developed optimizer was linked with eigenvalue analysis and load prediction software. The stiffness and inertia properties of the cross section were optimized by changing the dimensions of the cross section. The analyses were subjected to constraints on blade mass, 1st mass moment and composite ply-up restrictions. A tailored blade for minimum vibration and reduced control loads was obtained while significantly reducing the design time.

1.12. Objective

In most of the above studies, the spanwise location of the lumped masses were taken as design variables. The chordwise offsets of the lumped masses are expected to produce coupling between the torsional and flapwise bending response of the blade. Vibration reduction can be derived by taking advantage of these couplings. The current study employs three non-structural lumped masses with variations in both spanwise and chordwise directions to reduce the vibratory hub loads. The underlying mechanisms behind this reduction of the vibration are investigated. VAST, a multi-physics, multi-model simulation program, is used as the helicopter comprehensive analysis. Optimization is carried out within the Remote Component Environment (RCE) which is an in-house developed workflow-integration tool. The operating condition is a low-speed forward descent case.

2. Introduction to VAST

This chapter describes VAST and its features, and the tasks which can be achieved with VAST. It also includes the general structure of VAST and describes the generic trim, it's algorithms and configuration, and their visualization methods

2.1. VAST (Versatile Aerodynamic Simulation Tool)

The Institute of Flight Systems of the German Aerospace Center (DLR) together with the Institute for Software Technology are developing a new framework for low and medium fidelity simulation of rotary wing aircraft to address the predictive accuracy in the highly complex field of helicopter simulation. These codes are called comprehensive codes, because they encompass a multitude of disciplines. Single aircraft components or even only certain aspects of those components are described with very specialized numerical models which can be large or only a few lines of code. On the other hand, models might be used that encompass multiple aircraft components in a certain discipline. Moreover, a wide range of fidelity is required to support different simulation goals like conceptual and preliminary design, flight mechanics, real-time flight simulators, coupling with high fidelity methods and detailed aeromechanic simulation. These unique requirements call for an extremely versatile framework which on the other hand allows for a high degree of specialization in the configuration, calculation and analysis procedures. To address this need in a modern future proof way and to push the boundaries of current comprehensive rotorcraft simulation VAST is being developed. This drives the modular and parametric nature of the code.

VAST is a multi-physics, multi-model simulation program with a very modular and generic approach. The architecture is strictly divided between simulation framework and the actual implementation of physics. Though it is for helicopter aeromechanic calculations but the Simulation Core, the User Interface, the Configuration, the simulation framework are also developed parallelly so that it could be used for any numerical simulation field requiring multi-model-simulation. Apart from physical models there are tasks implemented in the framework both completely generic like the transient solution through time and specific to the use-case like the free-flight trim of a helicopter.

The main design idea is to divide a simulation problem into different disciplines and to model their respective sub-problems in separate models which are then connected and simulated in conjunction with each other. All sub-models are formulated in a generic state-space-form with input, output and states as well as dynamic and output equation.

2.2. Working on VAST

The modules containing different aspects of the system or numerical modeling of different physical phenomena, often have different ways of communication with the rest of the code. This makes it much harder to understand the code and to implement new functionalities.

The idea in VAST is to keep a strict separation between physical models and all other aspects of the code and to provide one generic interface to all physical models, thus making the code as modular as possible. To do this all models are set up in such a way, that they appear as state-space-models to the outside (see Figure 13). Moreover, all models inherit from a generic state-space-model enforcing an identical structure and interface. This way all models can be handled in the same way and truly generic solution procedures can be implemented.

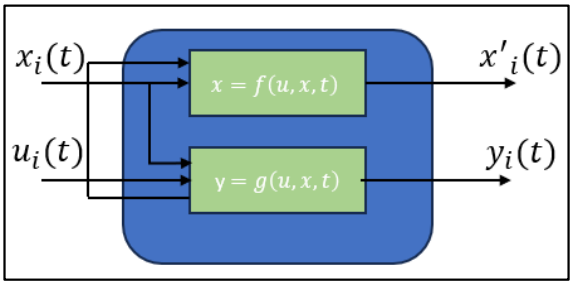

Figure 13. VAST Generic State-Space-Model

2.3. Features of VAST

- Generic simulation core with automatic gradient calculation and connection, calculation with arbitrary couplings
- Entire configuration based on xsd/xml scheme using TIXI for reading and writing as well as code generation
- Simple GUI for configuration, calculation and visualization
- Arbitrary rigid mechanical systems with open loop structure (MBS)
- Wind tunnel trim of a rigid MBS rotor
- Flexible rotor blade as a generic finite element component for linear 1D FE structures. A Euler-Bernoulli beam model and Houbolt & Brooks blade model are available, the latter is only verified for blades without axis offsets. Additionally, the Beam Advanced Model (BAM) which useful to create an overview to extract more information about the particular field, it is currently available for frequency analyses of beams with straight neutral axes that are colinear with the pitch-control axis. BAM has been verified for blades with axis offsets and pre-twist. Model reduction via a modified Craig-Bampton approach is available. Thus, flexible blades can either be computed with the full or reduced system
- Semi-empirical analytical model for unsteady air loads (currently only for NACA23012)
- Look-up-table models of steady polars for airfoils and air loads that are applied at a single point (like fuselage or empennage loads)
- Semi-empirical fuselage-rotor interference model
- Blade geometry: arbitrary blade planforms can be input via different formats. Arbitrary sweep, anhedral, chord and twist can be prescribed
- Configuration in the GUI: configurations can be built up by adding models to a tree-view and modifying the parameters. This is done directly from the xsd-file describing all VAST input parameters and sub-models. No change in the GUI is required when new functionality is added to the simulation. It is directly checked via test calls to the solver if a configuration is valid in terms of model in-/outputs. All in-/outputs are displayed vis-a-vis making it easier to track errors in the configuration. A basic model graph displays the connection between models. This will be enhanced to show the type of connection and further information
- 3D view in GUI-configuration and animation: This view currently displays the position and orientation of the reference frames defined in the configuration for communication between the models. Basically, all reference-frame definitions that make it in the output-vector of the solver are displayed. The geometry of rotor blades is automatically generated from the configuration and displayed in a simplified form (just the planform in 3D with constant thickness). This gives a good first impression of the configuration and a means to check axis-orientation and the like. It is also possible to display arbitrary geometries (provided as wavefront obj-file) and connect them to markers of an MBS body
- Campbell diagrams (natural frequencies of the system over a varying system parameter like rotational speed of the rotor)
- Python API. VAST can be imported into python scripts and its high-level methods controlled from the script. Batch processing in custom python scripts is the main target of the current API version. Apart from running the high-level methods like "initialize", "run_simulation_- steps", etc. The user can access and manipulate the current states, outputs and parameters. The API will be expanded in the future e.g. for external coupling applications

2.4. Limitations of the VAST

- Analytical airfoils: the only real airfoil currently available is NACA23012. All other airfoils described by unsteady analytical polars for the Leiss model available in S4 still need to be transferred to VAST. This is true for both rotorcraft and wind turbine airfoils
- Blade geometry: while arbitrary blade shapes can be configured and computed, the feature has not been thoroughly tested yet. Most verification and validation cases use straight rectangular blades, so this feature is still experimental.

2.5. General Structure of VAST

This section describes the general architecture of VAST. It starts with the main components and details how they work together. All components are grouped around the Core. It contains the non-linear system description and a solver that handles coupling between VAST Generic State-Space-Models and the integration through time.

The main components of VAST are depicted in Figure 14[41]. A Graphical User Interface (GUI) is employed to set up the system to be simulated and to specify simulation parameters and cases. This information is stored in input files which are then used by the actual simulation, here called Simulation Framework, to perform the simulation and produce output files. These output files are used by a post processor or visualization engine to produce visual results of the simulation. The GUI controls and monitors the calculation which can either be run as a predefined batch process or in an interactive mode.

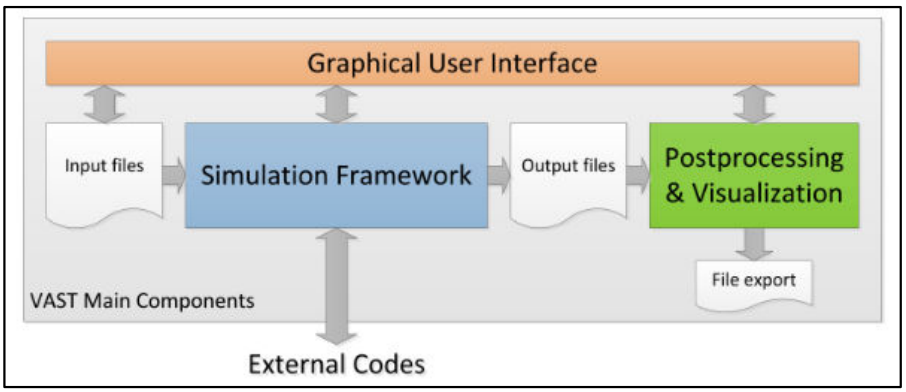

Figure 14. Main Components of VAST [41]

Figure 15 describes the Simulation Framework which divided in four parts. Initialization handles the configuration of the system to be simulated, reads all input data and provides all parts of the framework with parameters needed for execution. The Core does just that, perform a non-linear time simulation with the specified model and the specified simulation parameters. System Analysis contains all methods of analysis that either use the non-linear time simulation or operate on the model directly (e.g. Eigen analysis). Everything time marching with the full system is handled directly in the block Core. The process control essentially executes a batch script with a list of tasks for the calculation (e.g. initialize the system → perform a trim → perform time simulation with given inputs → etc.).

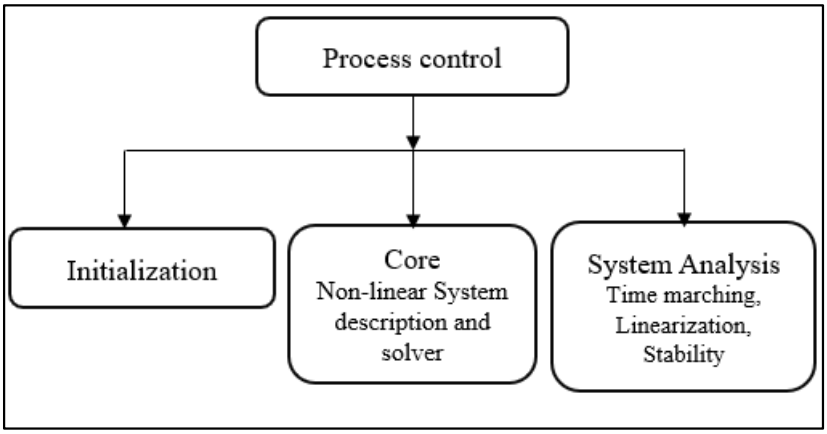

Figure 15. VAST Simulation Framework

2.6. Generic Trim in VAST

In helicopters, trim is used to maintain the position by adjusting the aerodynamic forces on the control surface. Simple configuration for a generic trim case (wind tunnel or free-flight). This tries to find valid values for a set of unknowns to fit the trim objectives to their target values. Here the difference between wind tunnel trim and free flight trim is that, in wind tunnel trim the study of aerodynamic interaction will be extracted while performing the experiment in a test tube with the support of induced airflow, whereas in case of free flight trim the study will be performed without any external control.

Unknowns ("trimValues") are: * initial vehicle orientation, e.g. "Euler angles" of the rotorcraft * parameters of models (in particular rotor controls)

Objectives ("trimObjectives") are: * changes in the flight path of the vehicle, e.g. vehicle acceleration * outputs of models (averaged for time-varying systems)

Additional parameters ("trim Parameters"): * flight-path parameters (flight speed, flight-path angle, turn rate and sideslip angle).

In addition, one can choose "equilibrium States" which defines both unknowns and objectives and which tries to find states that do not change from one timePeriod to another (e.g. reach a possibly periodic equilibrium). Supports time-varying as well as quasi-stationary systems. The resulting solver state is set to the state at the end of the trim simulation. So, the simulation time is advanced by (startUpPeriods+1) * time Period. And the model parameters are set to the values calculated by the trim.

A trim sweep can be configured by setting numStepsInTrimSweep to a value greater than 1. The start and end values of the trim objectives and flight-path parameters can be configured in the respective sub-nodes.

2.7. Trim Algorithms and their configuration parameters in VAST

For this section, we assume that a system with possibly several models (structure, aerodynamics, etc.) has been set up, and either a free_flight_trim or wind_tunnel_trim task has been added to the simulation_steps. We will describe what actually happens if such a trim task is executed and how this is influenced by the configuration parameters.

In general, during the trim task an iterative optimization method is used to find trim values which lead to fulfilled trim objectives. That is, starting with initial trim values, the algorithm performs a time simulation with exactly these parameters and checks if the trim objectives are already fulfilled. If this is not the case, the trim values are adapted and another simulation is performed. This procedure is pursued until the trim objectives are fulfilled (or a different stopping criterion is reached). Each of the simulations consists of several steps, which are described in the following:

Initialization: In general, an arbitrary number of simulation_steps can be executed before the trim task, for example, a time_evolution. The parameter reinitialize of the trim task can be used to configure (re-)initialiazation in the beginning of each of the simulations that is performed during the trim task. If reinitialize is set to true, all states of the models are set to their initial states and the simulation time is also set to zero. If, on the other hand, reinitialize is set to false, the states are not modified and the final states and the final simulation time from the previous simulation_step are reused. Note that if the trim task is the first simulation_step, then reinitialize=true is required!

The Time Simulation: Itself After the initialization, a VAST time simulation is performed. For this, with the timePeriod parameter of the trim task, one can prescribe the actual simulation time (e. g., one rotor revolution), which corresponds to the time frame, in which the trim objectives need to be finally fulfilled. Additionally, one can set the startUpPeriods parameter to obtain a simulation time of (1+startUpPeriods) * timePeriod, where the trim objectives need only be fulfilled in the last period. Note that this time simulation uses the same time integration solver as, for example, a time_evolution task.

Measurement of the Trim Objectives: the simulation is performed for a simulation time of (1+startUpPeriods) * timePeriod and the measurement of the trim objectives is only performed in the last time period, which is often called the measurement revolution if the time period corresponds to one rotor revolution.

Within this measurement period, different operations are performed on the different types of trim objectives to determine the actual objective function, which is then handed over to the optimization method. For the trimObjectives, the average of the respective output variable is calculated over the measurement period, which should then reach the target value. This is done to account for, for example, vibrations, which may have great influence on a measurement of the output at only one point in time. For the equilibriumStates, the difference of the values at the end and the beginning is calculated and the target value for this quantity is zero (corresponding to the desired periodicity of the variables). Finally, for the vehicleFlightPath, the flight path variables are transformed to the states of the system (which are, therefore, taken as initial values for the time simulation), and the actual objective for the optimization is an acceleration of zero (which is computed again as the average of the acceleration over the measurement period).

Stopping Criterion: The optimization iteration needs to be stopped at some point, ideally after the iteration yielded convergence. To obtain a guaranteed stopping of the iteration (even if it doesn't converge), one can specify the parameter maxTrimIterations, which makes the iteration stop after the specified number of iterations.

The goodness of fit of the current trim values is measured with the residual sum of squares of the trim objectives. As one cannot expect that the trim objectives are fulfilled exactly (that is, the residual is exactly zero), the parameter maxTrimResidual of the trim task can be provided. The iteration will stop, assuming that it has converged, once the residual is below this threshold.

2.8. Modal Analysis, Campbell Diagram and Equilibrium in VAST

Modal Analysis

Perform a modal analysis around the current state of the system. This is achieved by linearizing the system and computing all eigenvalues of the linearized system matrix. The resulting pairs of eigenvalues together with the eigenfrequencies are output to the configured filename.

Implementation: The modal analysis task performs a linearization around the current state of the system and calculates the eigenvalues and eigenvectors of the resulting linearized system matrix.

Campbell Diagram

Perform a sweep over a range of parameter values. For each step, put the system in an equilibrium and perform a modal analysis around the equilibrium state. The resulting eigenfrequencies for each step are output.

Implementation: The Campbell diagram task performs a sweep over the given relative range for the given parameter variable. For each value of the parameter variable, an equilibrium is calculated and a modal analysis is performed. The resulting damped eigenfrequencies for each step are output to a file for visualization.

Equilibrium

Equilibrium tries to find a static or dynamic equilibrium for all states in the system. The states of the system are modified to find an equilibrium, that is to say where the states become constant (static equilibrium) or periodic (dynamic equilibrium) If the period is 0 a static equilibrium (x where dx=0) is the goal. With a non-zero period the dynamic equilibrium, defined as x(t_0) = x(t_end), is to be found.

Implementation: The equilibrium task uses the generic trim and its "equilibriumStates" functionality in the background. Essentially the trim object "equilibriumStates" is applied to all states of the system.

3. Basic Helicopter Theory context to the VAST models

This chapter deals with the physics of a helicopter by giving the theoretical context to the VAST models.

The origin and orientation of a coordinate system itself must also be specified with respect to another system. Technically, this is usually done in a recursive way forming a tree structure. The root will most likely be an inertial frame of reference

When dealing with aircraft it is reasonable to follow a common convention which defines a set of base coordinate systems. The coordinate system convention in VAST is chosen to comply with the standard DIN 9300 [41]. The most relevant frames of reference are listed below

3.1. Pitt-Peters three state dynamic inflow model & Generalized Dynamic Wake Model

Pitt and Peters (1981) developed a three state first harmonic dynamic inflow model. This model consists of three first order differential equations. Chen [41] correlated several sets of test data with theory and he stated that the Pitt/Peters first harmonic inflow model works well overall. Because of its better correlation with test data and less computational cost, this model is widely used in the rotorcraft aeromechanical studies. This model is well suited for preliminary design optimizations, trim calculation, vehicle and rotor stability analysis, control law development, real time flight simulations and estimation of handling qualities. However, this model is inadequate for vibration analysis, since the model has only three states and first harmonic azimuthal variation.

Chengjian He (1989) developed the Generalized Dynamic Wake theory for the lifting rotors. It is an extended version of Pitt-Peters dynamic inflow model. This model is a finite state inflow model. Number of inflow states from the model can be varied by choosing appropriate number of harmonics and highest power of radial polynomials. Since the model can be able to predict the higher harmonic induced velocity distribution, it can be used for aeroelastic and vibration studies.

Both Pitt-Peters dynamic inflow and generalized dynamic wake models do not include the wake distortion effects, such as wake bending and wake spacing effects, which are essential for better prediction of vehicle responses during transient maneuvering flight conditions, particularly the off-axis responses.

3.2. Computational Fluid Dynamics, Prescribed Wake & Dynamic wake distortion model

CFD discretizes the entire volume into small cells in which the Navier-Stokes-Equations are solved. It is a first-principles approach, and therefore by definition suited to capture all physical effects in sufficient detail. In reality CFD also uses derived models to reach acceptable calculation times and to improve stability. Most notably here are turbulence models. CFD is much more compute intensive than Free Wake (around 106−9 more expensive) and is therefore reserved for detailed investigations of single flight cases and mostly to steady flight conditions.

Prescribed Wake is similar to Free Wake insofar as it is also based in a 2D grid deformed in 3D space. This deformation however is precalculated by a set of parameters derived from global flight parameters and disk loading. This prescribed deformation is then used to calculate influence coefficients on the rotor blades, making the calculation much less compute intensive. Prescribed wake models are roughly as compute expensive as the Generalized Dynamic Wake Model. It needs a trimmed entire rotor revolution to compute the influence coefficients, therefore it is not suited for maneuvering flight. It can however better capture blade vortex interaction and its results are for isolated forward flight cases comparable with Free Wake. A good description of the prescribed wake model can be found in [34]. This model is mentioned only for completeness, currently there is no implementation of it in VAST.

This model is a refined version of generalized dynamic wake model. The refinements are inclusion of wake curvature, non-uniform wake spacing, and composition of straight and skewed wake. These refinements give the significant improvements in the prediction of off-axis responses during climb, transition from steady to transient maneuver and extreme transient maneuvering flight conditions (pull up/down). This model is mentioned only for completeness, currently there is no implementation of it in VAST. These three models are need to be further developed to obtain better results.

4. The Approaches of Rotor Induced Vibratory Load Reduction

The rotor induced vibrations can be handled in two ways which can be identified as direct and indirect approaches. In the direct approach, the blades were designed or modified for the minimized rotor hub vibratory loads. The vibratory loads consist of inertial and aerodynamic loads. These are caused due to complex aerodynamic environment and blade response to oscillatory loads. Instead of direct load calculation the indirect approach is more beneficial from the relationship between the blade natural frequencies and aerodynamic excitation frequencies. These direct and indirect approaches were referred to as “Hub Loads Minimization” and “Natural Frequency Separation” respectively.

4.1. Natural Frequency Separation

The calculation of blade natural frequencies is critical in the determination of blade dynamic characteristics. The problem of finding the natural frequencies is a free vibration problem for rotating beams and the knowledge on the blade equations of motion is essential. The helicopter main rotor blades are characterized by slender, elastic beams which are usually subjected to high-speed angular rotation. Generally, the blades are twisted; the mass and stiffness values are variable over the blade. The elastic axis and center of mass are usually separated with an offset and application of non-structural masses is quite common. In addition to the problems arising from the blade geometry, even at usual operating conditions the blades are under a significant centrifugal force field which varies over the blade. This centrifugal force has stiffening effect on the blade and dominates the dynamics of the blade. The dynamic analyses of blades show considerable difficulties because of all these geometric, elastic and inertial effects.

The interaction of natural frequencies with the excitation frequencies is critical. In rotorcraft studies, it is a common practice to identify frequencies in non-dimensional form. Then the fundamental frequency in non-dimensional form is defined as 1/rev. The rotor harmonics are the aerodynamic excitation at frequencies, these are termed as integer multiples of rotor angular speed (n(1/rev) = n/rev, n=1,2,3…) [3]. The main causes of the excitation are the cyclic pitch input, velocity distribution over rotor disc due to forward flight, blade stall, motion induced loads and the vortex interactions between blades and fuselage. Any coincidence of these aerodynamic excitations and the blade natural frequencies causes excessive vibrations and load amplification on the rotor and these rotor vibrations are transferred to the fuselage [1].

Natural frequency separation method is very advantageous if the rotor aerodynamic model is unreliable for high frequency load computations or computationally too expensive. The excitation frequencies are irrespective of the magnitudes of the aerodynamic loads and are always the integer multiples of the rotor angular speed (Ω). Since the natural frequencies of blade should not come close to those excitation frequencies, the blades can be designed for reduced vibrational level by natural frequency separation approach [1]-[2]. Since blade natural frequencies are evaluated for the in-vacuo condition, the solution of the rotor aeroelastic motion is not required.

4.2. Hub Loads Minimization

The next method of vibration reduction is calculating the hub loads which performs with an overall rotor evaluation when aerodynamic and structural dynamic models are included. The complex dynamic and aerodynamic operation environment of the helicopter rotor was explained in Section 1.2. The blades respond to oscillatory aerodynamic loads which in turn cause oscillatory blade motion. This interaction between excitation and response generates the dynamic loads at the blade root. The dynamic blade loads of each rotor blade root which are integrated at the rotor hub and the overall dynamic loads at the rotor hub which excites the body are responsible for the helicopter vibration. Figure 16 presents the representative rotating and non-rotating coordinate systems and related force and moments.

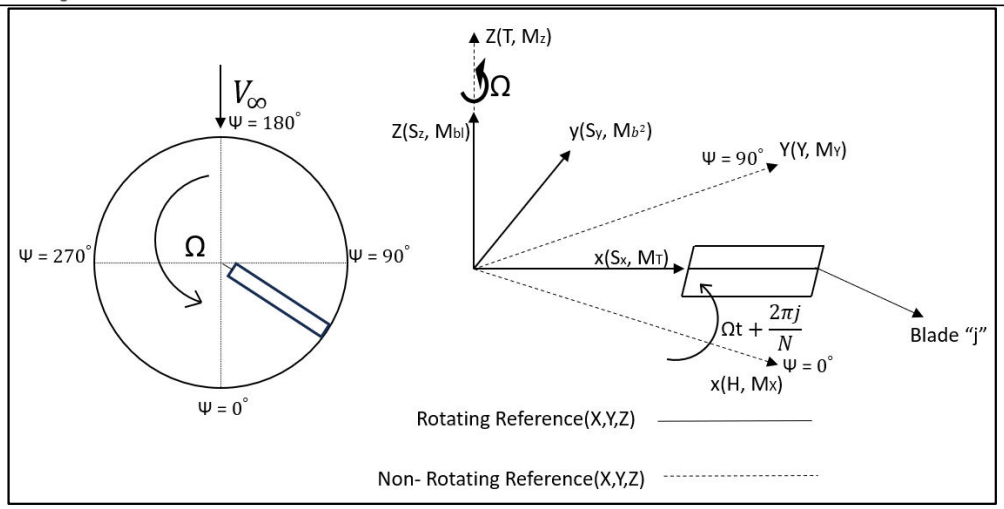

Figure 16. Hub and Blade Reference Frames and Vertical Shear Forces

Rotating coordinate system rotates with blade whereas the hub reference frame is fixed on the rotor hub as given in Figure 16. In order to define the loads transferred at the hub, rotating blade loads including three force and moment components should be integrated at the hub origin. H, Y and T are representing forces acting at longitudinal, lateral and vertical hub and M_X, M_Y and M_Z are representing the reference system of rolling, pitching and yawing hub moments at the non-rotating hub. Force and moment contributions from each blade root in the rotating hub reference frame are identified by S_X, S_Y, S_Z and M_X, M_{bF}, M_{bI} respectively. S_X, S_Y, S_Z represent the shear forces and M_T, M_{bF} and,M_{bI} represent the moments in radial, flap wise and chordwise directions. The subscripts 0, n_c and n_s defines the steady, n^{th} cosine and n^{th} sine contributions respectively. Total hub loads are calculated by integrating these blade root loads at the rotor hub. For illustration of the hub loads calculation procedure, if blade vertical root shear and vertical hub forces of Figure 28 is considered [3];

$$T = NS_{Z0} + \sum_{n=1}^{\infty}\left\{\sum_{j=1}^{N}\left[S_{Znc}\ cos\, n\left(\Omega t + \frac{2\pi j}{N}\right) + S_{ZnS}\ sin\, n\left(\Omega t + \frac{2\pi j}{N}\right)\right]\right\} \quad 3$$

By using proper trigonometric summation;

$$T = N\left\{S_{Z0} + \sum_{j=1}^{N}\delta_{n(kN)}\left[S_{Znc}\ cos\, n(\Omega t) + S_{ZnS}\ sin\, n(\Omega t)\right]\right\} \quad 4$$

where k is integer, N is number of blades, n is integer harmonics. The Kronecker delta formulation is;

$$\delta = \begin{cases} 1; i = j \\ 0; i \neq j \end{cases}$$

Since other force and moment components are also vector quantities, similar integration and trigonometric properties yields the set of hub equations [3];

$$H = \frac{N}{2}\left\{-S_{Y1s} + \sum_{n=1}^{\infty}\delta_{n(kN)}\left[\left(S_{Y(n-1)s} - S_{Y(n+1)s}\right) cos\, n(\Omega t) + \left(S_{Y(n-1)c} - S_{Y(n+1)c}\right) sin\, n(\Omega t)\right]\right\} \quad 5$$

$$Y = \frac{N}{2}\left\{S_{Y1s} + \sum_{n=1}^{\infty}\delta_{n(kN)}\left[\left(S_{Y(n-1)s} + S_{Y(n+1)s}\right) cos\, n(\Omega t) + \left(S_{Y(n-1)c} + S_{Y(n+1)c}\right) sin\, n(\Omega t)\right]\right\} \quad 6$$

$$T = N\left\{S_{Z0} + \sum_{n=1}^{\infty}\delta_{n(kN)}\left[\left(S_{Znc}\right) cos\, n(\Omega t) + \left(S_{ZnS}\right) sin\, n(\Omega t)\right]\right\} \quad 7$$

$$M_X = \frac{N}{2}\left\{M_{bF1s}\sum_{n=1}^{\infty}\delta_{n(kN)}\left[\left(-M_{bF(n-1)s} + M_{bF(n+1)s}\right) cos\, n(\Omega t) + \left(M_{bF(n-1)s} - M_{bF(n+1)s}\right) sin\, n(\Omega t)\right]\right\} \quad 8$$

$$M_Y = \frac{N}{2}\{-M_{bF1s} + \sum_{n=1}^{\infty}\delta_{n(kN)}[(-M_{bF(n-1)s} - M_{bF(n+1)s})\cos n(\Omega t) + (-M_{bF(n-1)s} - M_{bF(n+1)s})\sin n(\Omega t)]\} \quad 9$$

$$M_Z = -N\{-M_{b10} + \sum_{n=1}^{\infty}\delta_{n(kN)}[(M_{bInc})\cos n(\Omega t) + (M_{bIns})\sin n(\Omega t)]\} \quad 10$$

When the blades are uniform and equally spaced, some frequencies of the blade root loads are cancelled at the hub. Direct delta function of n and kN in Equations 5-10 shows that for equally spaced rotors, the rotor acts as a filter and only harmonic loads at integer multiples of rotor (kN/rev) speed are transferred to hub as vibratory loads. For the vertical hub loads, only kN/rev harmonics of blade loads contribute to kN/rev vertical hub loads whereas for in-plane loads (kN-1)/rev and (kN+1)/rev harmonics of blade loads contribute to kN/rev hub loads.

The lower the vibratory loads, the smaller the level of fuselage vibrations. This describes the dynamic loads at the frequency which are integer multiples of blades per cycle (kN/rev) can be decreased. Generally higher frequencies have very small amplitudes therefore it is usually enough to consider N/rev loads [32].

Due to the periodic nature of the rotor, it is common practice to represent hub loads by sine and cosine components and functions of rotor angular coordinate (Ψ). Therefore, the hub load equations in time domain can be formulated in rotor disc angular coordinate domain for a rotor with N blades at N/rev frequency as;

$$H(\Psi)_{N/rev} = H_{N,c}\cos N\Psi + H_{N,s}\sin N\Psi \quad 11$$

$$Y(\Psi)_{N/rev} = Y_{N,c}\cos N\Psi + Y_{N,s}\sin N\Psi \quad 12$$

$$T(\Psi)_{N/rev} = T_{N,c}\cos N\Psi + T_{N,s}\sin N\Psi \quad 13$$

$$M_X(\Psi)_{N/rev} = MX_{N,c}\cos N\Psi + MX_{N,s}\sin N\Psi \quad 14$$

$$M_Y(\Psi)_{N/rev} = MY_{N,c}\cos N\Psi + MY_{N,s}\sin N\Psi \quad 15$$

$$M_Z(\Psi)_{N/rev} = MZ_{N,c}\cos N\Psi + MZ_{N,s}\sin N\Psi \quad 16$$

The three force and moment parameters of vibratory hub loads excite the fuselage at every kN/rev frequency. The fuselage response to these vibratory loads causes the vibration [32] of the airframe. In addition to airframe structure other components in the non-rotating frame such as avionics, flight crew and passengers and payload are also affected.

Compared to “Natural Frequency Separation method”, “Hub Loads Minimization” is more advantageous of the contribution of vibratory loads that are of aerodynamic origin. The exact values of the loads to be minimized provide better physical insight into the problem.

With the above observations and discussed processes for vibration reduction, passive method of placing tuning masses aft the elastic axis is followed to optimize the vibration index. To continue the optimization process, the VAST tool is integrated into RCE. It is a workflow-integrated environment where the multiple tools are integrated.

The features of the RCE and the initial approach of performing the optimization process with a small experiment of integrating multiple tools and the final results for reducing the vibration loads at the hub are discussed in the upcoming chapters.

5. Introduction to RCE (Remote Control Environment)

RCE (Remote Component Environment) is an open-source software. RCE creates, manages and executes complex in calculation and simulation workflows for engineers, scientists and others. RCE workflow consists of predefined inputs and outputs connected to each other. A component can be a tool for data access,a simulation tool, or a user-defined script. Connections define which data flows from one component to another also predefined components with common functionalities, like an optimizer or a cluster component. Additionally, users can integrate their own tools. RCE instances can be connected with externally through networking component where the tools can be executed locally or on remote instances of RCE (if the component is configured to allow this). Using these building blocks, use cases for complex distributed applications can be solved with RCE.

5.1. Features and Major Software involved in RCE

Integration: The central feature of RCE is Coupling of external tools into workflows. Once the tool gets integrated then it can be accessed through standardized inputs and outputs. Through configuration most tools can be integrated.

Automation: By the connection of outputs of one tool to inputs of other tools, the tools get coupled. Once all required data of inputs are available, the tool gets executed by RCE. Execution of tool and workflow is automated which requires no user interaction.

Data Management: The result data of a design, analysis, or simulation task is essential for the engineers and scientists. The tools of the workflow generate the results while execution. Later, all the data will be collected by RCE of the respective tools and presents it through graphical viewer.

Collaboration: Multiple tools are involved in simulation tasks, design or complex analysis which requires multiple tools and they also located at different sites. In order to support collaboration, tool servers and clients are connected through RCE into a peer-to-peer network.

The major software involved in RCE are:

CPACS: Common Parametric Aircraft Configuration Schema (CPACS)is a software which defines and describes the data format for the development and design to the air transportation systems. It also enables to exchange information between the design tools. To simplify the integration, RCE has special wrapping functionality which uses CPACS as their inputs or outputs.

TiGL: The TiGL Geometry Library (TiGL) is a geometric representation of aircraft based on the CPACS file description. The library consists of TiGL Viewer, through which the inception of constructed geometry can be enabled through an interactive user interface. The configuration of RCE to use the TiGL viewer, displays geometries used in a workflow.

IslandViz: The Island Visualization (IslandViz) is a tool for visualization and also explores the modular software systems through virtual reality. Representation of IslandViz of every module as unique island on a virtual table. Through this, user can overview regarding the complexity of an OSGi based software system by exploring its modules as well as the dependencies interactively.

5.2. Workflow Components and their functions in RCE

Workflow components are either tools that are integrated by users or are provided by RCE supplying multi-purpose functionality.

- Data: Database
- Data Flow: Input Provider, Output Writer, Joiner, Switch
- Evaluation: Optimizer, Design of Experiments, Parametric Study, Converger, Evaluation Memory
- Execution: Script, Cluster, Excel
- XML: XML Loader, XML Merger, XML Values
- CPACS: TiGL Viewer, VAMPzero Initializer

A connection needs to be created between the sending workflow component and the receiving one. For that purpose, workflow components can have so called inputs and outputs. A connection is always created between an output and an input. Data is sent as atomic packages which are not related to each other (there is no data streaming between workflow components). Supported data types are short text, Integer, Float, Boolean Referenced data types (The actual data is stored in RCE's data management and only a reference is transferred).

The Referenced data types are File, Directory and other data types like small table where at the table values a,b,c,d are restricted to values of type Short Text, Integer, Float, Boolean (primitive data types) as well as File and Directory, Vector is one-dimensional "Small Table" (one column) restricted to values of type Float, Matrix which is a Small Table restricted to values of type Float

A creation of connection will be created between an output and an input if:

- The data type of the output is the same or convertible to the data type of the input.
- The input is not prior connected to another output.

Note that data from an output can be sent to multiple inputs, but an input can just receive data from a single output [40].

The execution of workflows is data-driven. As soon as all of the desired input data is available, a workflow component will be executed. the input data is defined by the component developer, the tool integrator, and/or the workflow creator. The workflow component developer and tool integrator decide which options are allowed for a particular workflow component. The workflow creator can choose between those options at workflow design time. The following options exist:

Input handling:

- **Constant**: The value won't be consumed during execution and will be reused in the next iteration (if there is any loop in the workflow). The workflow will fail if there is more than one value received, except for nested loops: All inputs of type Constant are reset within nested loops, after the nested loop has been finished
- **Single (Consumed):** The input value will be consumed during execution and won't be reused in the next iteration (if there is any loop in the workflow). Queuing of input values is not allowed. If another value is received before the current one was consumed, the workflow will fail. This can guard against workflow design errors. E.g., an optimizer must not receive more than one value at one single input within one iteration.
- **Queue (Consumed):** The input value will be consumed during execution and won't be reused in the next iteration (if there is any loop in the workflow). Queuing of input values is allowed.

Execution constraint:

- **Required**: The input data is required for execution. Here, the input has to be connected for an output.
- **Required if connected**: The input data is not required for execution (e.g., if a default value will be used as fall back within the component). Thus, the connection for the input to the output is specifically required if there is a connection.
- **Not required**: The input data is not required for execution. If it is connected to an output, the input value will be passed to the component if there is a value available at the time of execution. Values at inputs of type Not required cannot trigger component execution except if it is the only input defined for a component. Note: With this option, non-deterministic workflows can be easily created. Use this option carefully. If in doubt, leave it out.

Workflow components can be coupled to loops. A loop must always contain a so-called driver workflow component. Driver workflow components (group "Evaluation") are: Optimizer, Design of Experiments, Parametric Study, Converger. The responsibilities of a driver workflow component in a loop are to Send values to the loop and receive the result values and finish the loop based on some certain criteria.

When workflow components of a loop fail due to it couldn't compute any results for the inputs received but works normally. In this case, it sends a value of type "not-a-value" with the specified cause to its outputs which finally are received by the driver workflow components as results or it crashes for an unexpected reason. In this case, the workflow engine sends values of type "not-a-value" with the specified cause as results to the driver workflow component.

5.3. Integrating External Tools in RCE

RCE comes with a number of components that already allow to create rather large and complex workflows. Technically it is possible to create a workflow only with the components with RCE, as the external tools can be callable through the Script-component. Maintaining such a workflow will, however, prove quite cumbersome. However, in all instances of the Script-component in the workflow must be individually configured, as there exists no possibility in sharing configuration between component instances. Finally, while components can be shared among a network of RCE instances [40] this sharing does not extend to configuration values such as the script of a Script-component. Overall to simplify the creation, sharing, and maintenance of workflows consisting will call to external tools, RCE allows for the integration of such external tools and define as user-defined components.

To integrate an external tool, the tool must:

- callable through command line,
- be a non-interactive mode which is called via command line
- consists of input provided by environment variables, command line arguments, or files

When executing an integrated tool, a certain directory structure is created in the chosen working directory. This structure depends on the options chosen in the integration wizard. The two options that matter are "Use a new working directory each run" and "Tool copying behavior".

Root Working Directory: This is the directory to choose in the "Tool Integration Wizard" as "Working Directory" on the "Launch Settings" page.

Config Directory: In this directory, the configuration file that may be created by the tool integration will be created by default. The configuration files can be created from the properties that are defined for the tool on the "Tool Properties" page.

Input Directory: Every input of type "File" and "Directory" are copied here. They will have a subdirectory that has the same name as the name of the input (e.g. the input "x" of type "File" will be put into "Input Directory/x/filename").

Output Directory: Every output of type "File" and "Directory" can be written into this directory. After that, the use of the placeholder for this directory to assign these outputs to RCE outputs in the post execution script. To write, e.g., the output directory into an output "x" of type "Directory" the following line in the post execution script would be required: ${out:x} = "${dir:output}"

Tool Directory: This is the directory to the location of the actual tool. If the tool should not be copied, it will be exactly the same directory that you choose, otherwise it will be the same as the chosen directory but copied to the working directory.

Working Directory: A working directory is always the location, where all the other directories will be created. If the option "Use a new working directory on each run" is disabled, this will always be the same as the "Root Working Directory". Otherwise, a new directory is created each run (the name will be the run number) and is the working directory for the run.

The tools are executed by using a command line call on the operating system via the execution script. When the tool finished executing (with or without error), its exit code is handed back to the execution script and can be analyzed in this script. If in the script nothing else is done, the exit code is handed back to RCE.

When there is an exit code that is not "0", RCE assumes that the tool crashed and thus lets the component crash without executing the post script. Using the option "Exit codes other than 0 is not an error" prevents the component from crashing immediately. With this option enabled, the post script will be executed in any way and the exit code from the tool execution can be read by using the placeholder from Additional Properties.

5.4. Example of integrating multiple tools in RCE and performing Optimization

This section explains the workflow of the project and a detailed description of the software RCE and its process of integrating and working with multiple tools. The idea behind the integration of Fusion 360 for CAD modelling and FreeCAD for FEA of the CAD model imported from Fusion 360 to perform Optimization where the Objective is to retain minimal material which is sufficient to withstand the stresses.

The objective function is to minimize f from (17);

$$f = \sigma_{yield} - \sigma_{von\ mises} \quad 17$$

Where σ_{yield}, the yield stress of steel of compression load is 250 MPa and $\sigma_{von\ mises}$ is calculated through the FEA from FreeCAD

The design constraints are:

$$Constraint\ 1 = Length\_value - \frac{d}{2} - x \quad 18$$

$$Constraint\ 2 = Breadth\_value - \frac{d}{2} - z \quad 19$$

$$Constraint\ 3 = x - \frac{d}{2} \quad 20$$

$$Constraint\ 4 = z - \frac{d}{2} \quad 21$$

Here length value is the length of the rectangular block which is 120 mm and breadth value is breadth of the rectangular block of 100 mm. Figure 17 describes the flow chart of the required process to optimize the required Design using multiple tools in RCE.

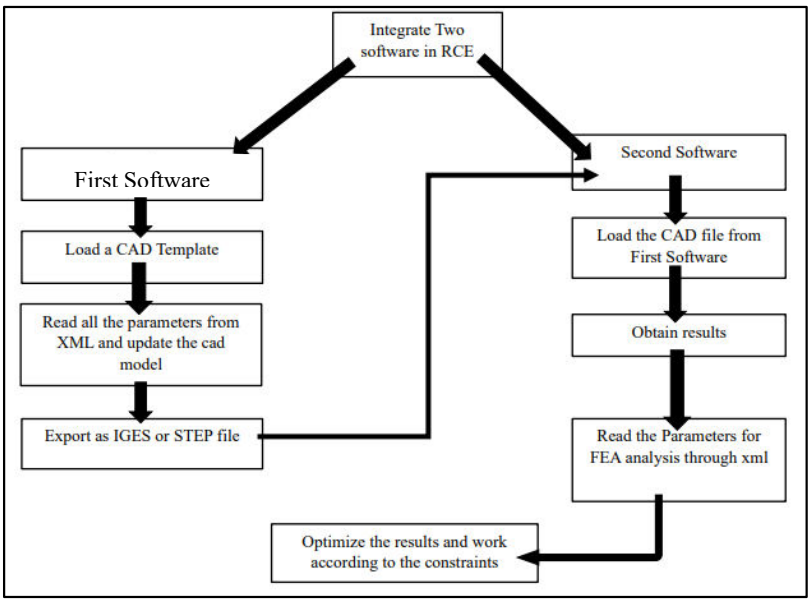

Figure 17. Flowchart describing the process of Optimization in RCE

Figure 18 describes the parametric CAD model automated through python using parameters from XML and exported as a STEP file

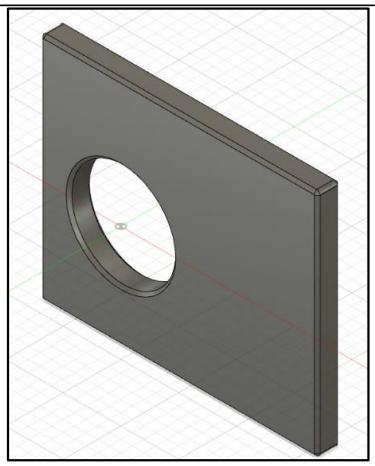

Figure 18. CAD Model Rectangular block with a hole

The STEP file is imported into FreeCAD and performs Finite Element Analysis through Macros by providing the material properties of Steel, meshing, fixed constraints and force constraints through the data from XML as presented in Figure 19.

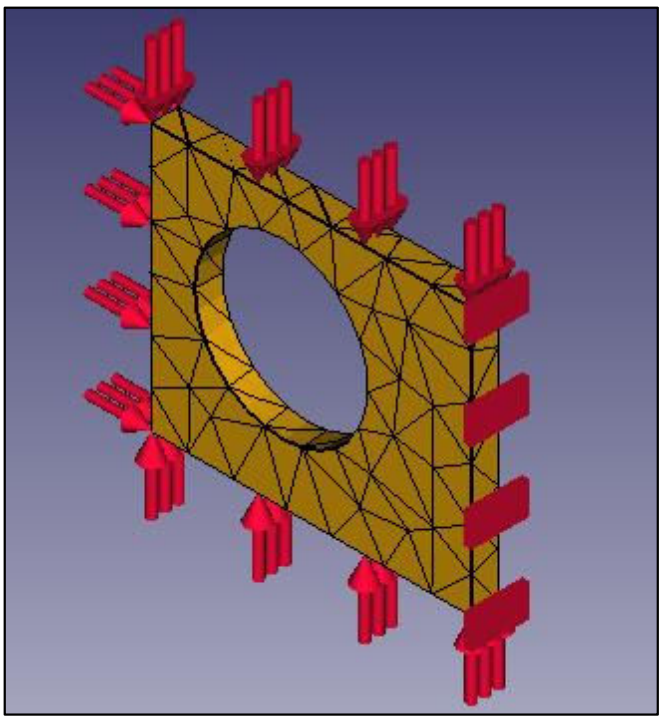

Figure 19. CAD model before Static Analysis

After the FEA the results are obtained, gets exported to an excel file presenting the maximum and minimum von-mises stress values through a plot focusing on Von Mises Stress Vs Nodes and the stress acting areas of the CAD model are presented in the FreeCAD tool which are presented from Figure 20 and 21.

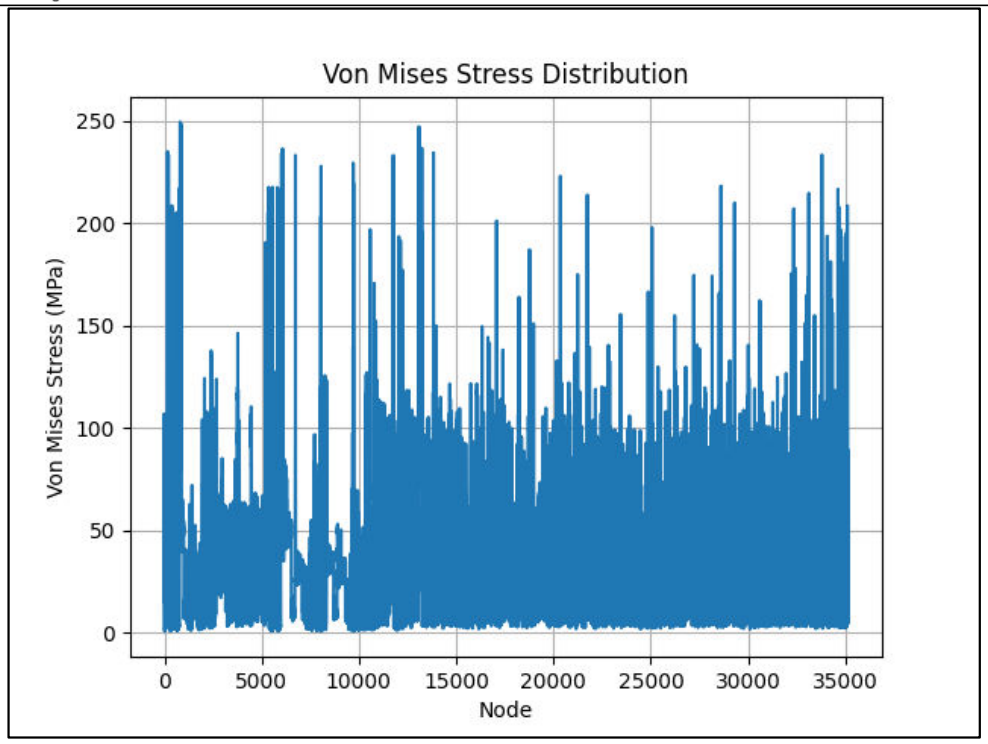

Figure 20. Plot representing Von Mises Stress Vs Node

Prior of integrating Fusion 360 and FreeCAD into RCE the process of designing the CAD model, performing and obtaining the results of FEA through automation works using batch files and then the test run has been performed by integrating the tools inside RCE, and obtained the optimized results. To obtain the best design parameters of the CAD model and minimize the objective function, both the tools are connected to Optimizer in RCE to perform the optimization process.

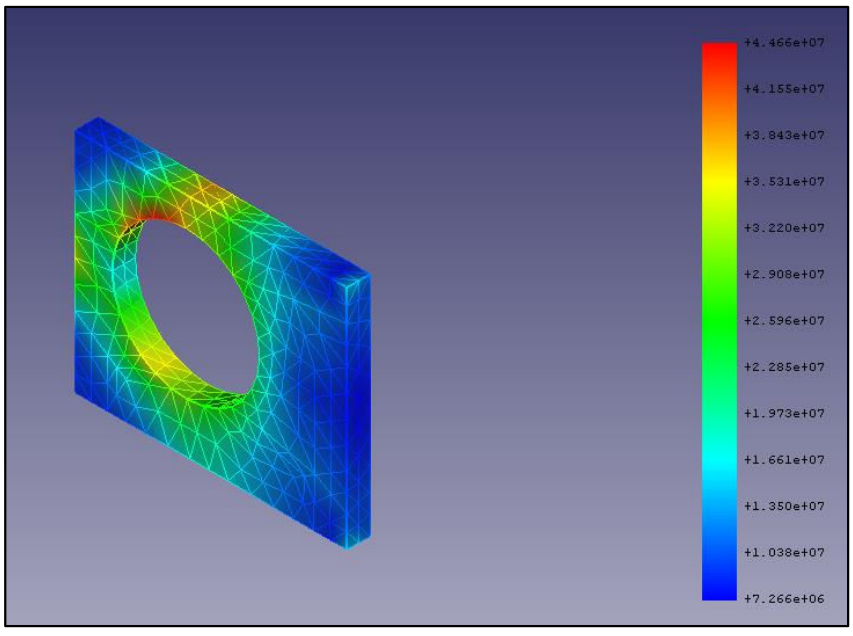

Figure 21. Von Mises Stress acting areas of the CAD model

Before integrating the tools in the workflow of RCE, the objective function, design variables and design constraints are given to the optimizer in RCE as shown in Figure 22.

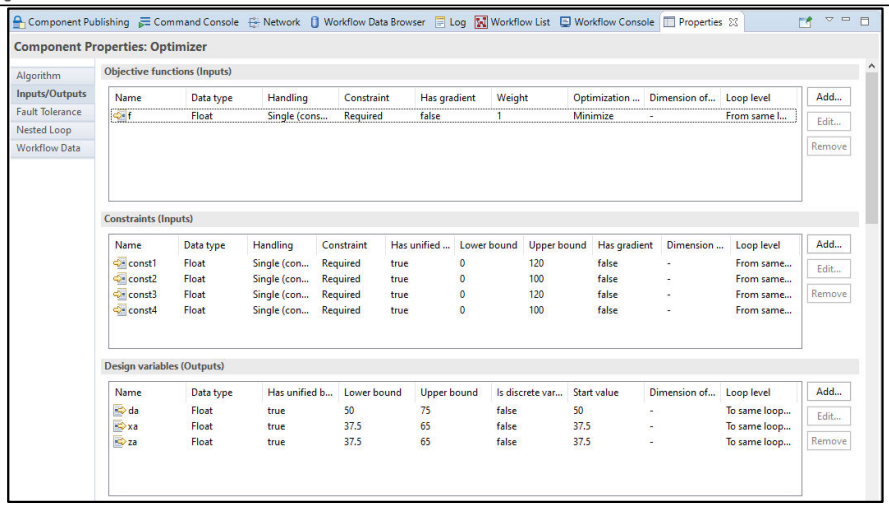

Figure 22. Component Properties of Optimizer

Then in the Script the constraints are calculated (from (*18*) to (*21*)) through the input values of d,x and z from the optimizer, then these values considers whether the constraint values are within the bound conditions and then passes the d, x and z as outputs to Fusion 360 which generates the CAD model. The design variables are: d- the diameter of the hole, x- the distance between the center of the co-ordinate system and the center of hole towards X direction, z- the distance between the center of the co-ordinate system and the center of hole towards Z direction

a) Integrating Tools in RCE

The integration of a tool in RCE is to be done through the following process:

1) Select integrate tool option in the tool bar, select 'Create a new tool configuration from a template' and select 'Create a new Common tool configuration' in choosing configuration of the tool in case of loading the software related to Aircrafts select 'Create a new tool configuration from a template'
2) Provide the title and description of the tool in the next section
3) In the next section provide the inputs and outputs for the tool,
    - In Fusion 360 d, x and z values are the float inputs coming from the script through which the CAD model has been generated and the outputs section Step file which is be imported to the FreeCAD is given to be provided
    - In FreeCAD the input is the step file which is coming from Fusion 360 and the output will be the float value of f which is stated in (*17*)
4) Later, in the launch settings section provide the path file including with the version and provide the working directory path folder and limit the parallel executions to 1 and select OK
5) In the next section there are three executions which are: pre-execution command, execution command and post execution command
    - For Fusion 360 the pre execution script consists of the python script, to create the CAD model according to the d, x and z values which updates in the XML, in the execution command the path of the batch file which triggers the Fusion 360 and creates the CAD model according to parameters in the updated XML and exports the model as STEP file and terminates automatically, in the post execution the exported STEP file will be sent to the targeted folder through which the FreeCAD can import the CAD model
    - For FreeCAD the pre execution is to import the STEP file into the FreeCAD, the execution command consists of the path of batch file which triggers the tool and performs FEA according to the material properties, force constraints and fixed constraints through XML and obtain the results of maximum von mises value and exits automatically by saving these results, in the post execution command there is a script to calculate the objective function equation and sends the f value as an output to the optimizer

6) The next step is to Save and Activate the tool, which is visible under User Integrated Tools in the palette window. Figure 23 presents the complete workflow of the integrated tool connected to each other and also to the optimizer.

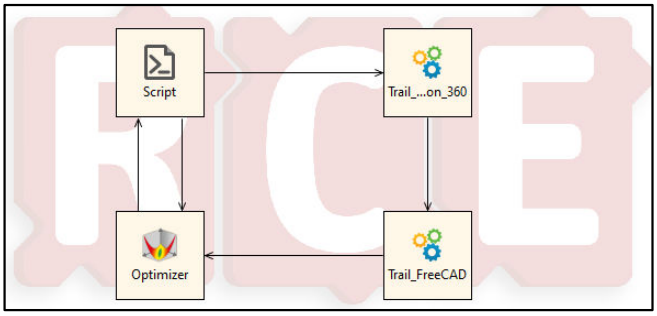

Figure 23. Workflow of integrated tools connected to the Optimizer in RCE

b) Optimization and Algorithms involved

For the example problem in RCE, Evolutionary algorithm and Single Objective Genetic Algorithm are used. The brief explanation of the algorithms are as follows;

Evolutionary Algorithm (EA): It is inspired by the process of natural evolution, helpful in finding solutions to complex optimization and search problems and in special this algorithm is particularly useful in dealing with non-linear, high-dimensional and noisy objective functions. The flowchart (Figure 24) explains the application of the algorithm in python script.

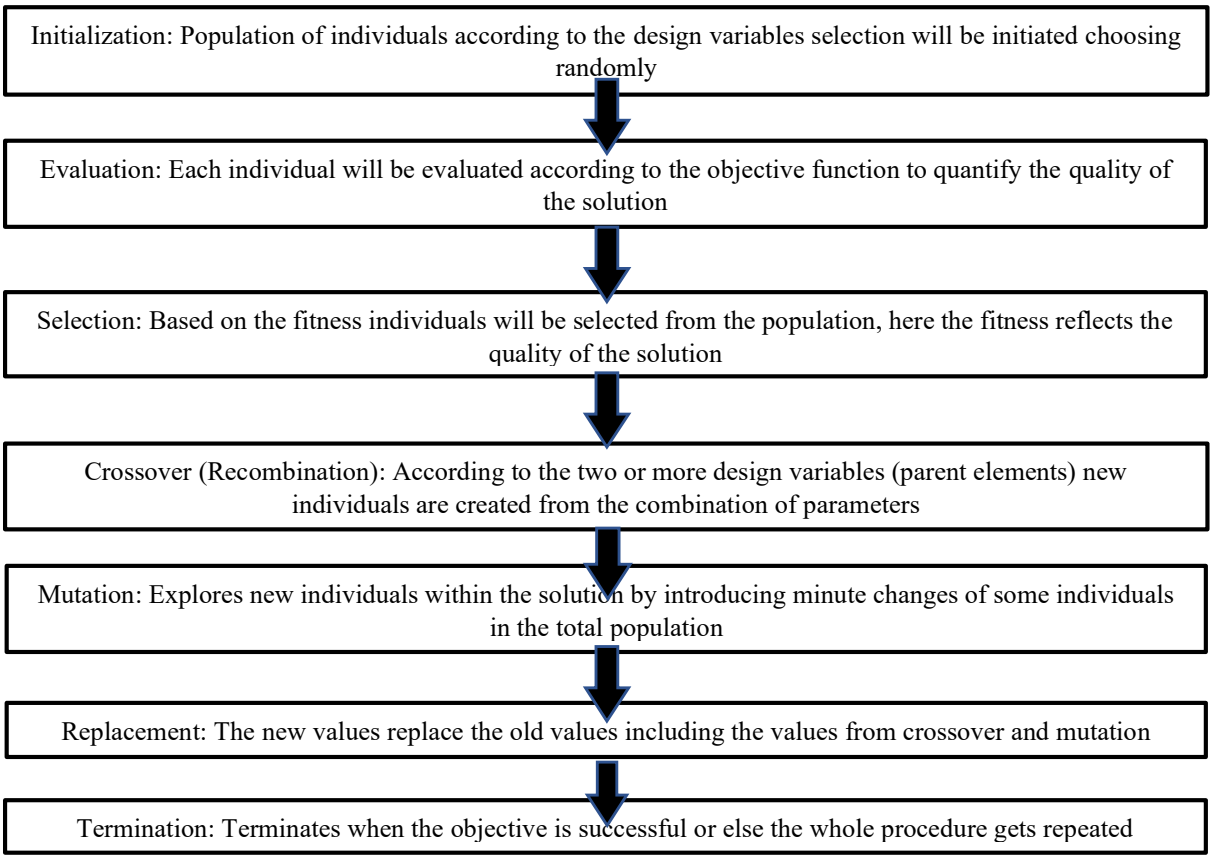

Figure 24. Flowchart describing the Application of Evolutionary Algorithm in Python

Single Objective Genetic Algorithm (SOGA): It belongs to the genetic algorithm and also the functioning is similar to evolutionary algorithm and this algorithm is specially designed to solve the function consisting single objective. The application of the SOGA in python is similar to the flowchart explained from Figure 24, consisting the Initialization, Evaluation, Selection, Crossover (Recombination), Mutation. Replacement and Termination.

Similarities between EA and SOGA:

Population Based

- Both algorithms work on the population based on individual solutions

Crossover

- Both algorithms use mutation and crossover operations in creating new individual solutions from the present population

Fitness

- In both algorithms the objective function evaluates the fitness of individual solutions, this helps in providing the quality of solutions

Global

- Both algorithms can perform optimization problems which has potential in finding the global optimal values specially for complex problems

Differences between EA and SOGA

Objective function

- Evolutionary algorithm can handle both Single objective and multiple objective functions
- Single Objective Genetic Algorithm is specially designed for the single objective for optimization problem

Termination Criteria

- In Evolutionary Algorithm termination depends on multiple factors like total number of iterations, computational budget and also achieving the satisfactory objective solution when multiple objectives are involved
- Single Objective Genetic Algorithm terminates as soon as satisfactory solution from optimization is generated

Representation

- Evolutionary Algorithm can be represented in multiple ways for individual solutions depending on the objective and the problem (For example; real valued vectors, binary strings, etc)
- Single Objective Genetic Algorithm is represented almost as same as EA but the specific concern is based on the solution of the optimization problem

5.5. Optimization results through in RCE by integrating desired tools

From the above sections, both Fusion 360 and FreeCAD are integrated inside RCE and connected to the Optimizer (as shown in Figure 23) to minimize the objective function were, $f = \sigma_{yield} - \sigma_{von\ mises}$

As the objective is scalar and only a single objective is used, the initial algorithm used for the optimization process is Single Objective Genetic Algorithm, the results of the optimization are discussed below:

a) Results of the optimization using Single Objective Genetic Algorithm

When Single Objective Genetic Algorithm is used for the optimization process, the total iterations were 410 and the best parameters were achieved at 356th evaluation the execution took 42928 seconds (approx.11 hours), the objective function value and the best parameters in attaining best objective function are presented below:

Best Objective Function: (f): 0. 117$\frac{N}{m^2}$

Best Parameters: Diameter of the hole(d): 65.416 mm, The distance in X-direction from centre of hole (x): 48.845 mm , The distance in Z-direction from centre of hole (z): 54.664 mm

By utilizing the best parameters the CAD model, the optimized CAD model after performing FEA in FreeCAD is presented below from Figure 25.

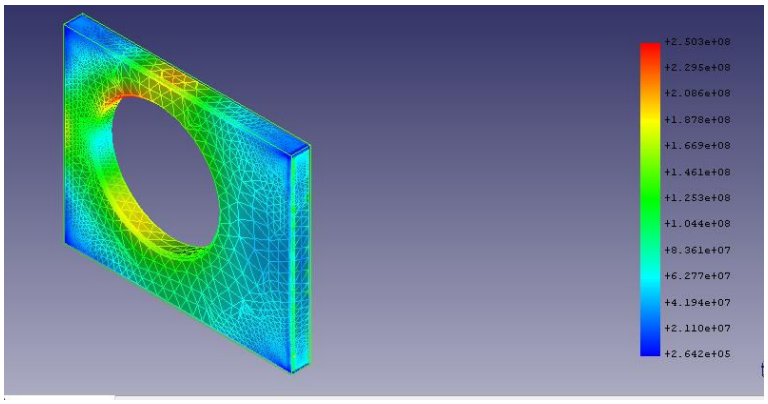

Figure 25. Optimized CAD model using Single Objective Genetic Algorithm

b) Results of the Optimizer using Evolutionary Algorithm

When Evolutionary Algorithm is used for the optimization process, the total iterations were 500 and the best parameters were achieved at 110th evaluation the execution took 95172.3 seconds (approx.26.43 hours), the objective function value and the best parameters in attaining best objective function are presented below:

Best Objective Function: (f): 0.7958 $\frac{N}{m^2}$

Best Parameters: Diameter of the hole (d): 52.202 mm, The distance in X-direction from centre of hole (x): 41.345 mm, The distance in Z-direction from centre of hole (z): 42.598 mm

By utilizing the best parameters into the CAD model, the optimized CAD model after performing FEA in FreeCAD is presented below from Figure 26.

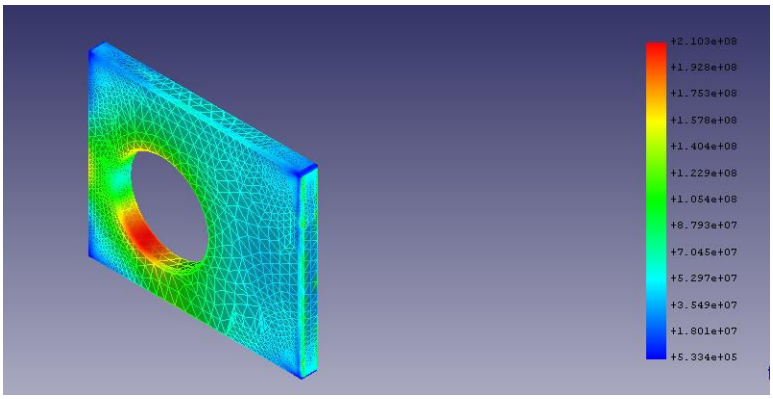

Figure 26. Optimized CAD model using Evolutionary Algorithm

From Figure 26, the area of stress acting region can be clearly observed, through the scaling at the right side it can be observed on the region where the highest von mises stress is acting.

By comparing both the results individually, the Evolutionary algorithm took more time to execute the results and also took more iterations when the objective function is achieved at 110th evaluation also when the best parameters of the Evolutionary Algorithm were applied individually outside RCE it didn't satisfy the objective function. Also, in compared with the Single Objective Genetic Algorithm, the best parameters were satisfying the given objective function condition.

The main motive of the optimization process is to remove the maximum material, where there will not be any deformation when the loads are applied, comparing with the diameter of the best parameters from Single Objective Genetic Algorithm of 65.416 mm and the given best parameter for the diameter using Evolutionary Algorithm is 52.201 mm. According to this comparison also, the best algorithm according to this given design constraints, variables and objective function Single Objective Genetic Algorithm is suggestable. In order to decrease the total time for the evaluation, the size of the population can be decreased when a single or else simple objective is being considered.

5.6. Limitations while using RCE

- The optimization still continues even though the constraint equations are not satisfied during Optimization in RCE, Figure 27 represents the errors occurred when the optimization continues without satisfying the constraints conditions

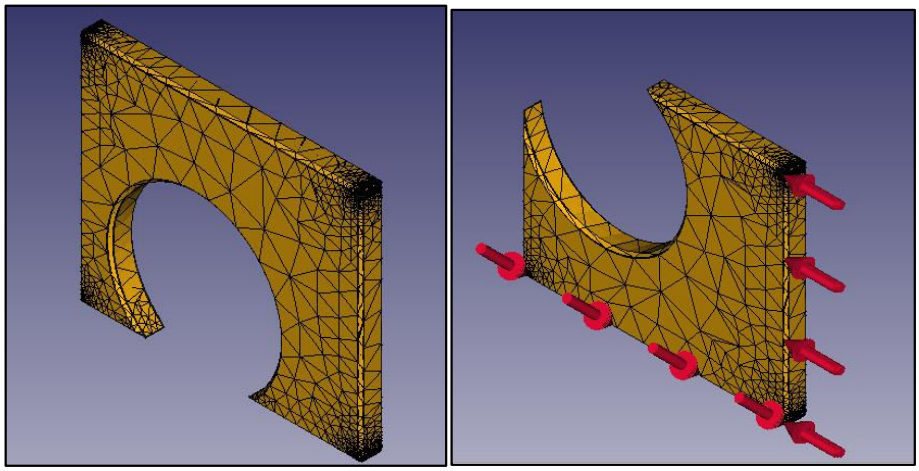

Figure 27. Performance of Optimizer in RCE without satisfying the constraint bound conditions

- RCE itself cannot trigger the tool and terminates after its execution, so batch files are to be used for integrating the tools and executing them
- The major issue faced while using RCE is that, the python is only compatible to Python 2.7, other library files and rest of the commands for scripting cannot be performed for developed versions in RCE
- RCE itself cannot trigger the tool and terminates after its execution, so batch files are to be used for integrating the tools and executing.
- The optimization process is time taking in providing the best parameters and best objective function
- The functioning of convergence is complex in RCE, as the results from optimizer are obtained there is no sign of convergence in the values, it need to be developed
- Networking process in connecting multiple systems is to be developed and to be easy in connecting the system within the environment
- RCE is only useful when multiple tools are involved and complex solutions are involved in the process, coming to the simple problems functioning outside RCE would be more simple

6. Results of Methods and Experiments performed to reduce vibrations on Rotor blade using RCE

This chapter deals with the design of experiments and optimization process involved to reduce the vibratory loads on the helicopter rotor blade.

Here VAST is the main tool to get the results in finding the vibration. To execute the VAST in optimization, the scripting is pre-written in the XML document which is termed as vast_config.xml, it contains all the data regarding the blade geometry, shaft tilt, wind velocity and other parameters responsible in operating the task in VAST. The process can be clearly explained through Figure 28 presenting the flowchart.

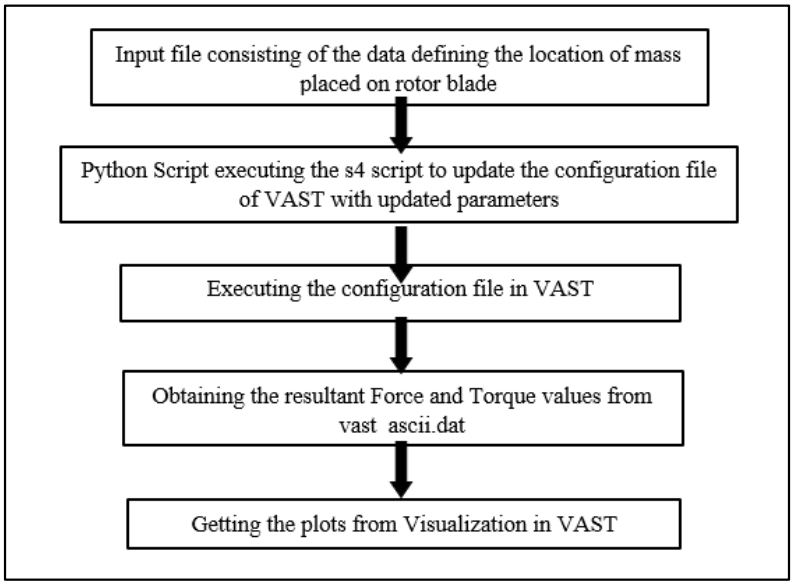

Figure 28. Flowchart describing the workflow process

After executing the vast_config.xml file inside VAST, it performs the task and export the results in vast_ascii.dat file where all the forces, torques acted on the rotor blade. Here, the major concern is the main constraint forces[N] acting on 3 Dimensions which can be termed as F_X, F_Y and F_Z and the main constraint torques [Nm] acting on 3 Dimensions which are termed as M_X, M_Y, M_Z. Figure 29 represents the plot obtained from the vast_ascii.dat files highlighting the curves of Forces and torques.

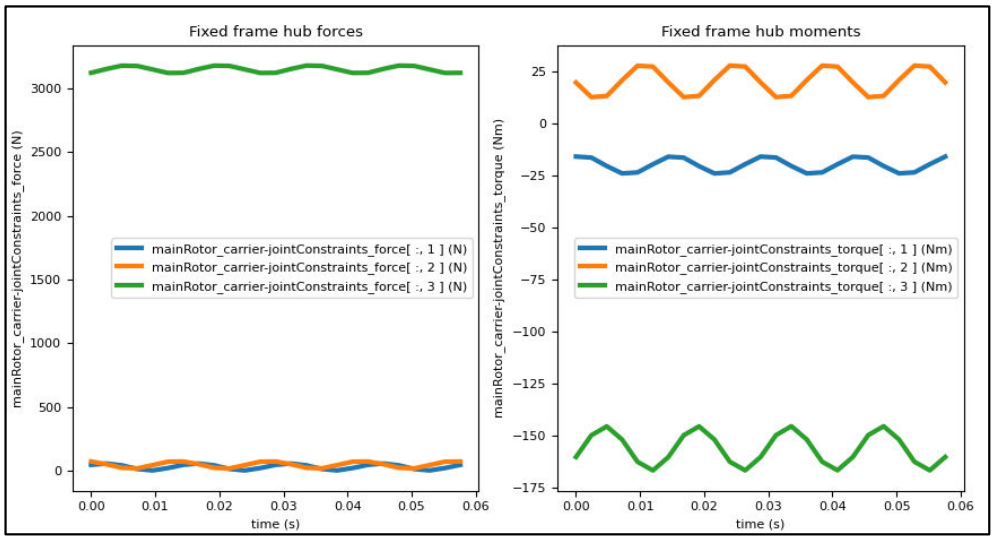

Figure 29. Plots describing the Fixed Frame Hub Forces(N) and Fixed Frame Hub Moments (Nm) Vs time(s)

Each force and torque provide the 25 set of values each are to be extracted with respect to the time provided in the vast_ascii.dat file. Using the set of values harmonic analysis is performed. The fourth harmonic's amplitude which is the root cause of the vibration on the rotor blade of each of the 3 hub forces and 3 hub torques is extracted so the calculated objective function is termed as follows;

$$f = \sqrt{(F_X^2 + F_Y^2 + F_Z^2)}[N] + \left(\frac{1}{R}\sqrt{(M_X^2 + M_Y^2 + M_Z^2)}\,[\frac{Nm}{m}]\right) \quad 22$$

Here R is the radius of the rotor blade, in this case the Radius is 2.0 m. The objective function is also termed as vibration index (VI).

There are various steps that are carried out to analyze the behavior of the vibration loads. Prior to the calculation of the objective function, there is an input file which plays a key role in evaluating the objective function when mass is placed on the rotor blade, this input file contains the data with locations of rotor blade[m], angle of twist[θ], amount of mass placed[kg], the moment of inertia[kg.m^2] when the mass is placed and the scalar value of which mass is placed on the elastic axis[m](if the mass is on elastic axis of the rotor blade it is zero when the mass is placed offset to the elastic axis the scalar value is to be noted at the space). This data is allotted from the 14th line to 32nd line on the input file. This data is primarily used during the whole experimentation process.

Later after updating the input file with the required data, then the script from S4 tool is used to combine these values into the vast_config.xml as this feature is not yet updated in VAST due to time constraints. By executing the script of S4 tool the data with the modified values gets updated into the VAST tool's XML file. Now, when the updated XML file gets executed in VAST extracts the data of force and torques which were mentioned above to perform the harmonic analysis and calculates the objective function.

6.1. Design of Experiments of mass 0.01 from varying locations for forward low speed descent flight condition

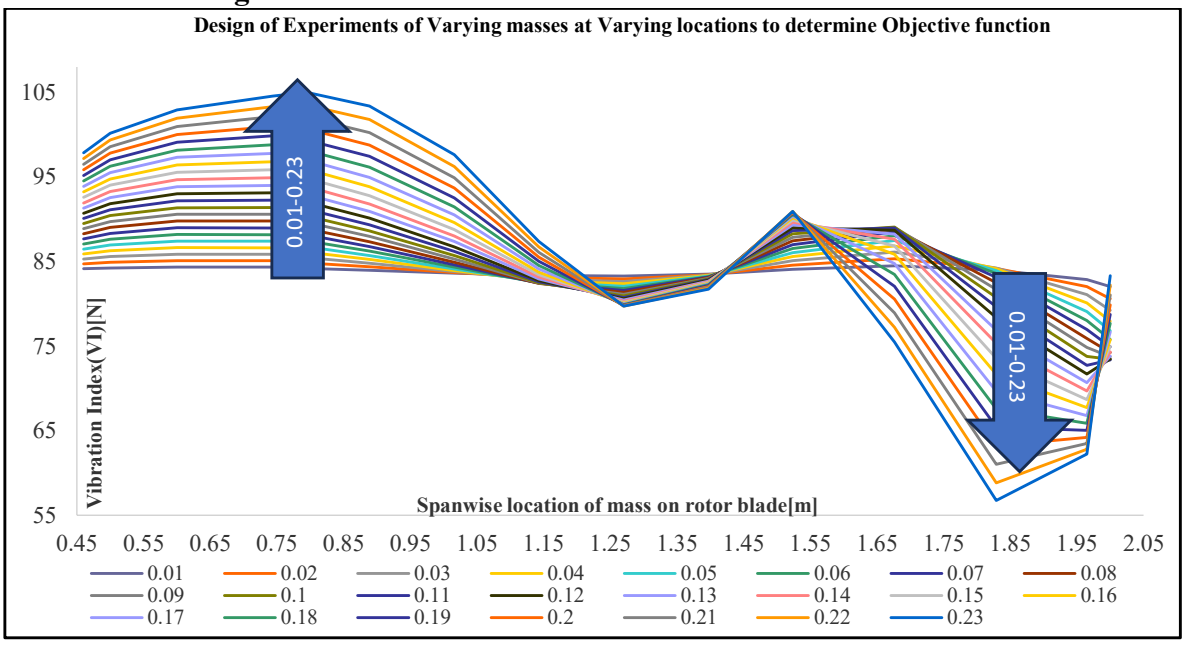

Figure 30. Vibration index when varying mass with 0.01 kg increment at varying spanwise locations

Figure 30 shows the results of one such DOE carried out by varying a single lumped mass from 0.01kg to 0.23kg (10% of blade weight) in incremental steps of 0.01kg. The spanwise location of the lumped mass is varied from 0.45m to 2m. It is seen that there is a clear trend in the variation of the vibration index with spanwise location of the lumped mass. This trend is maintained irrespective of the magnitude of the lumped mass. The maximum VI is observed at about 0.8m or 40% span of the blade while the least VI is observed at about 1.84m or 92% span. It is interesting to note that these two locations correspond to close to the antinode location of the second mode and the antinode locations of first, third and fifth mode, respectively.

6.2. DOE of distinctive mass at specified locations Offset to the elastic axis for forward low speed descent flight condition

For determining the effect of mass effect of mass effect on the vibration index, a new set of design of experiments were carried out by placing the single mass of 0.02kg,0.1kg and 0.23kg individually at 0.794m, 1.270m, 1.524m, 1.8229m and at 2.000m with offset range of (-0.0060) to (+0.0060). This offset range corresponds to -5% to 5% chord length .

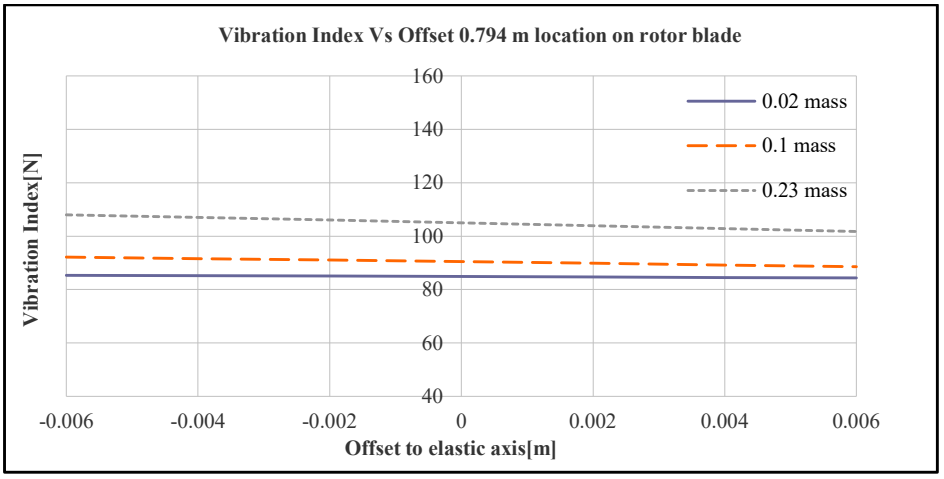

Figure 31. Vibration index Vs mass placed at 0.794m location at offset from elastic axis

Figure 31 and Figure 32 are the plots describing the behaviour of the objective function when the single masses of 0.02kg,0.1kg and 0.23kg are placed offset to the elastic axis ranging -0.0060 to +0.0060 on the helicopter rotor blade at 0.794m and at 1.270m away from the rotor hub. From the design of experiments, it was observed that irrespective of the magnitude of the mass, as it moves aft of the elastic axis to the fore, the objective function or the vibration index reduces in the inboard location (0.794m).

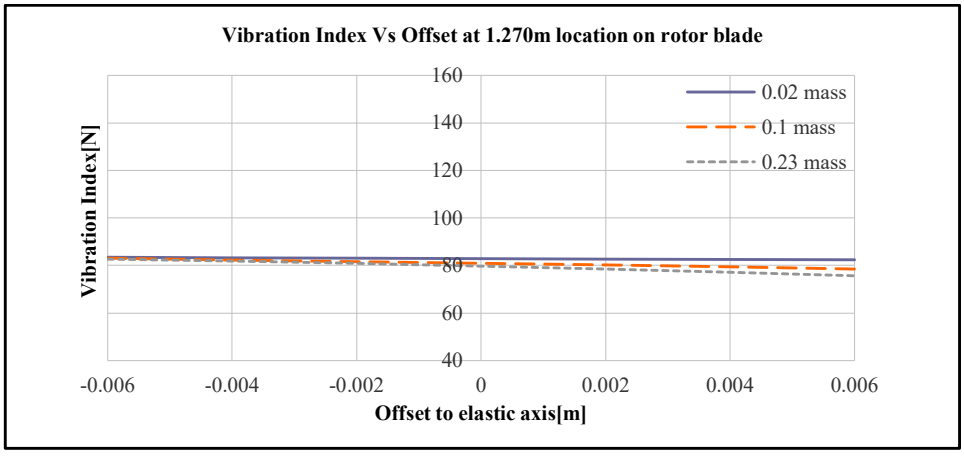

Figure 32. Vibration index Vs mass placed at 1.270 m location at offset from elastic axis

Figure 33 and Figure 34 are the plots describe the behaviour of the objective function when the single masses of 0.02kg,0.1kg and 0.23kg is placed offset to the elastic axis ranging -0.0060 to +0.0060 on the helicopter rotor blade at 1.524m and at 1.829m away from the rotor hub. From the design of experiments, it is observed that, irrespective of the mass magnitude, as the mass moves from aft of the elastic axis to the fore, the vibration index or the objective function increases.

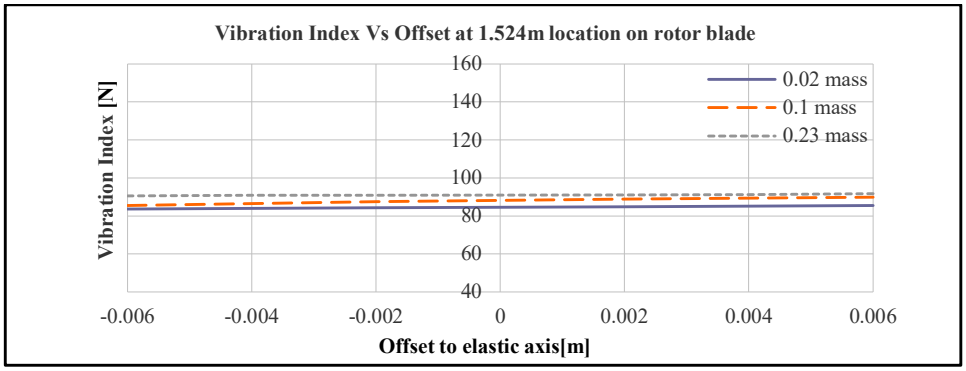

Figure 33. Vibration index Vs mass placed at 1.524 m location at offset from elastic axis

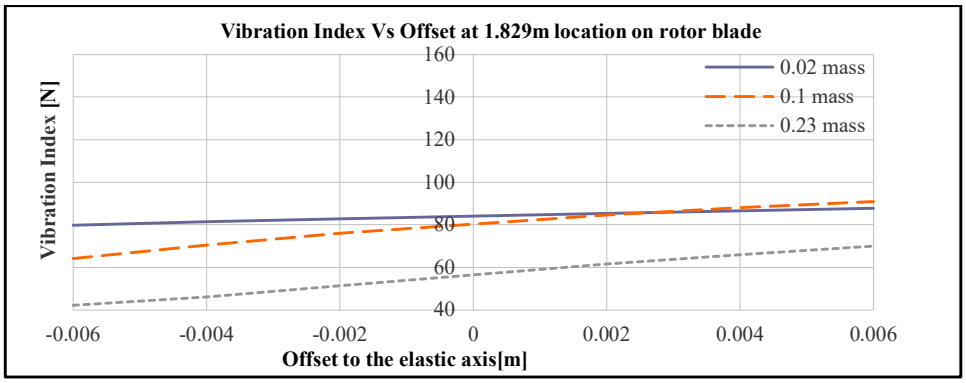

Figure 34. Vibration index Vs mass placed at 1.829m location at offset from elastic axis

Figure 35 is the plot that describes the behavior of the objective function when the single masses of 0.02kg,0.1kg and 0.23kg is placed offset to the elastic axis ranging -0.0060 to +0.0060 on the helicopter rotor blade at 2.0m away from the rotor hub which is at the tip of the rotor blade. The achieved objective function is more than the initial cases when 0.23kg mass is placed at the tip of the rotor blade. By observing all the plots where the mass is placed at varying locations offset to the elastic axis, it can be concluded that the minimal objective function is achieved when the mass is placed aft of the elastic axis and placed near the tip of the helicopter rotor blade.

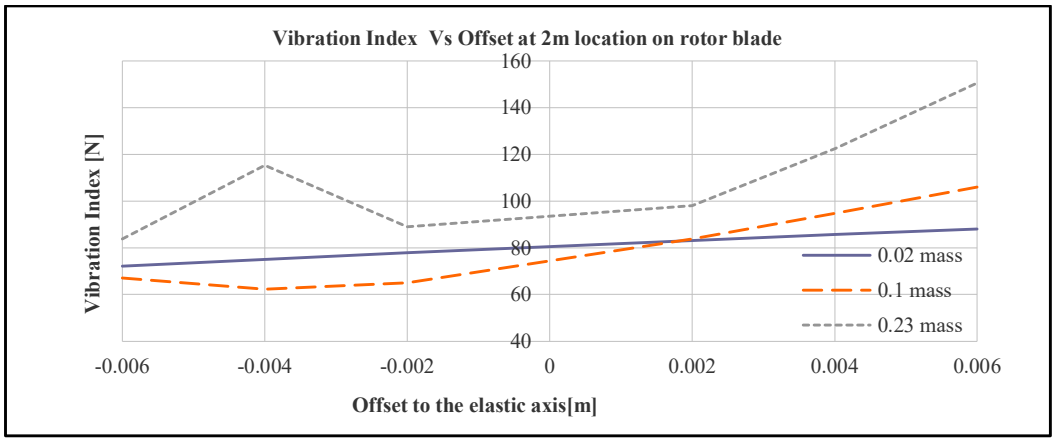

Figure 35. Vibration index Vs mass placed at 2m location at offset from elastic axis

6.3. DOE of twist angle without mass on rotor blade for forward low speed descent flight condition

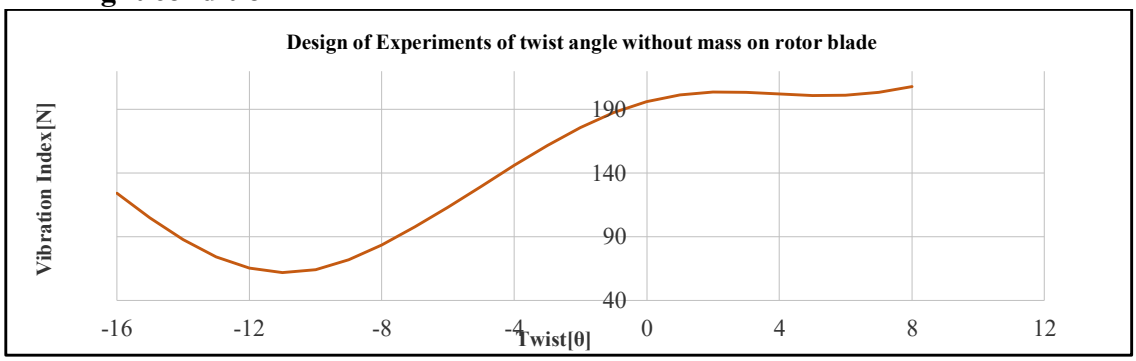

Figure 36.Plot describing the Vibration Index Vs Twist angle

Figure 36 represents the plot obtained when the design of experiments is performed to observe the objective function without mass on the rotor blade, the only design variable is twist angle whose lower and upper bounds are -16 and 8. Based on the plot the minimized objective function can be observed at twist angle of -11 and then there is a steady increase of objective function till twist angle of 8.

Before starting the optimization process to reduce the vibration by placing tuning masses on the helicopter rotor blade by minimizing the objective function, the baseline run has been performed to know the objective function value without masses placed, it ended up obtaining the baseline value of the objective function as 83.584N.

Later, the optimization experiments are carried out to observe the behavior of objective function when

i. three tuning masses are placed at three locations on rotor blade (case I),
ii. three tuning masses are placed offset to the elastic axis at varying locations (case II), and finally
iii. three tuning masses placed offset to the elastic axis at varying locations along with twist angle (case III).

All the experiments are carried out for forward low speed descent flight condition by fixing the wind speed value to 24.0 m/sec along Y-axis and providing the other axis values to 0.

6.4. Optimization in RCE to minimize the Vibration when 3 masses are placed at 3 different locations on the elastic axis of the rotor blade at Forward low speed Descent Flight condition

The first experiment for the optimization process is carried out by placing three tuning masses at varying locations at forward descent flight condition, consisting total of six design variables provided as inputs to the tool in RCE through optimizer under Single Objective Genetic Algorithm according to the bound conditions for the parameters from Table 1.

Parameters	Lower Bound	Upper Bound
Location 1[m]	0.46	2
Location 2[m]	0.46	2
Location 3[m]	0.46	2
Mass1 [kg]	0	0.05
Mass2 [kg]	0.025	0.0075
Mass3 [kg]	0.05	0.1

Table 1. Design Parameters for the Optimization

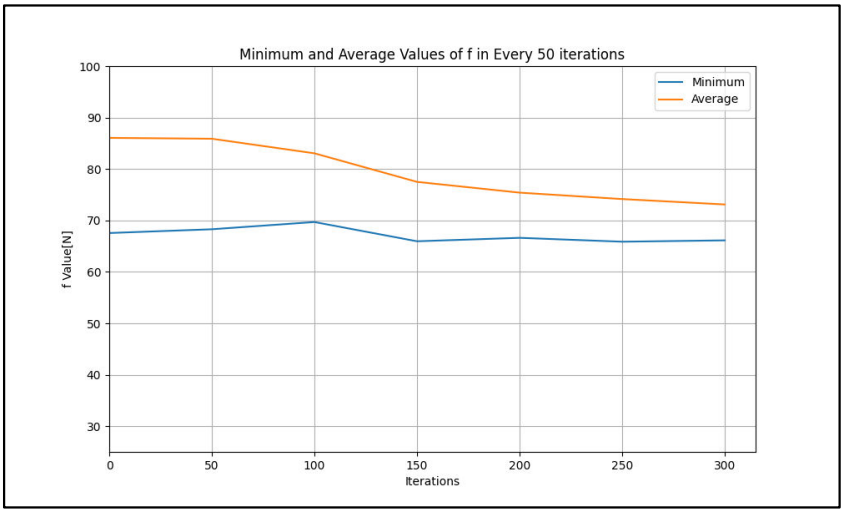

Figure 37. Convergence plot of Optimization to minimize the vibration when 3 masses are placed at varying locations

Later the optimization process has been performed and provides the objective function the optimized result which can be observed through Table 2 and Figure 37 is plotted against f value(objective function) and iterations which expalins the convergence of objective function during the optimization process.

Parameters	Results
Objective function	6.586e+001
mass1 [kg]	3.426e-002
mass2 [kg]	6.761e-002
mass3 [kg]	8.454e-002
location1 [m]	1.9650
location2 [m]	2.000
location3 [m]	1.6764

Table 2. Best parameters obtained through optimization process

6.5. Optimization in RCE to reduce vibrations on the helicopter rotor blade when 3 masses are placed at 3 different locations offset to the elastic axis at Forward low speed Descent Flight condition

The second experiment for the optimization process is carried out by placing three tuning masses offset to the elastic axis at varying locations at forward descent flight condition, consisting total of nine design variables(can be observed from Table 3) provided as inputs to the tool in RCE through optimizer under Single Objective Genetic Algorithm calculates the objective function and provided the optimized result which can be observed through Table 4 and Figure 38 is plotted against f value(objective function) and iterations which expalins the convergence of objective function during the optimization process.

Parameters	Lower Bound	Upper Bound
Location 1 [m]	0.46	2
Location 2 [m]	0.46	2
Location 3 [m]	0.46	2
Mass1 [kg]	0	0.05
Mass2 [kg]	0.025	0.0075
Mass3 [kg]	0.05	0.1
Offset 1 [m]	-0.0060	+0.0060
Offset2 [m]	-0.0060	+0.0060
Offset3 [m]	-0.0060	+0.0060

Table 3. Design variables for the second experiment

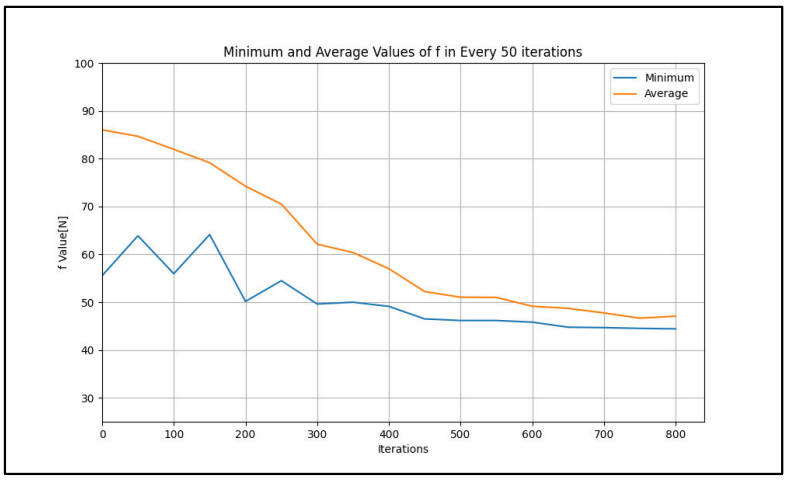

Figure 38. Convergence plot of Optimization to minimize the vibration when 3 masses are placed at varying locations offset to the elastic axis

Parameters	Results
Objective Function[N]	4.44E+01
Location 1[m]	1.6764
Location 2[m]	1.8290
Location 3[m]	1.9650
Mass 1[kg]	4.91E-002
Mass 2[kg]	7.42E-002
Mass 3[kg]	9.43E-002
Offset 1[m]	-5.63E-003
Offset 2[m]	-4.76E-003
Offset 3[m]	-5.11E-003

Table 4. Best parameters obtained through optimization

6.6. Optimization in RCE to reduce vibrations on the helicopter rotor blade when 3 masses are placed at 3 different locations offset to the elastic axis with varying twist angle at Forward low speed Descent Flight condition

The third experiment for the optimization process is carried out by placing three tuning masses offset to the elastic axis at varying locations and twist angle at forward descent flight condition, consisting total of ten design variables(see Table 5) provided as inputs to the tool in RCE through optimizer under Single Objective Genetic Algorithm.

Parameters	Lower Bound	Upper Bound
Location 1 [m]	0.46	2
Location 2 [m]	0.46	2
Location 3 [m]	0.46	2
Mass1 [kg]	0	0.05
Mass2 [kg]	0.025	0.0075
Mass3 [kg]	0.05	0.1
Offset 1 [m]	-0.0060	+0.0060
Offset2 [m]	-0.0060	+0.0060
Offset3 [m]	-0.0060	+0.0060
Twist [θ]	-16	8

Table 5. Design Variables for the third experiment

The calculated objective function and provided the optimized result which can be observed through Table 7 and Figure 39 is plotted against f value(objective function) and iterations which expalins the convergence of objective function during the optimization process.

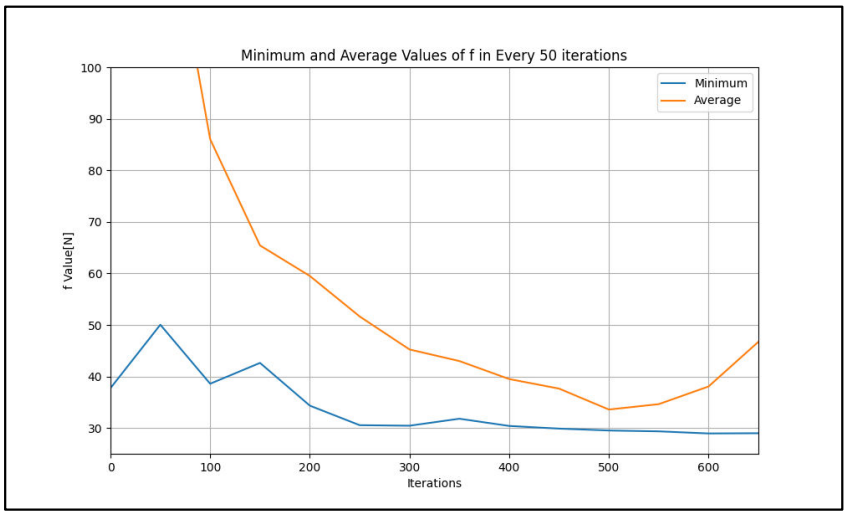

Figure 39. Convergence plot of Optimization to minimize the vibration when 3 masses are placed at varying locations offset to the elastic axis

Parameters	Results
Objective Function[N]	2.89e+001
Location 1[m]	1.6764
Location 2[m]	1.890
Location 3[m]	1.9650
Mass1[kg]	3.70e-002
Mass2[kg]	6.71e-002
Mass3[kg]	8.93e-002
Offset 1[m]	2.51e-003
Offset2[m]	5.81e-003
Offset3[m]	-3.81e-003
Twist[θ]	-11

Table 6. Best Parameters obtained through optimization process

After performing the experiments to minimize the vibratory loads when tuning masses are placed on the helicopter rotor blade using optimizer in RCE based on Single Objective Genetic Algorithm the minimization of the objective function has been achieved, in comparison with the base line objective function to all the three optimization processes there is a steady decline in objective function as can be clearly observed through Figure 40. From Figure 40 it can be clearly observed that the objective function has been decreased by 65.37% for the last experiment.

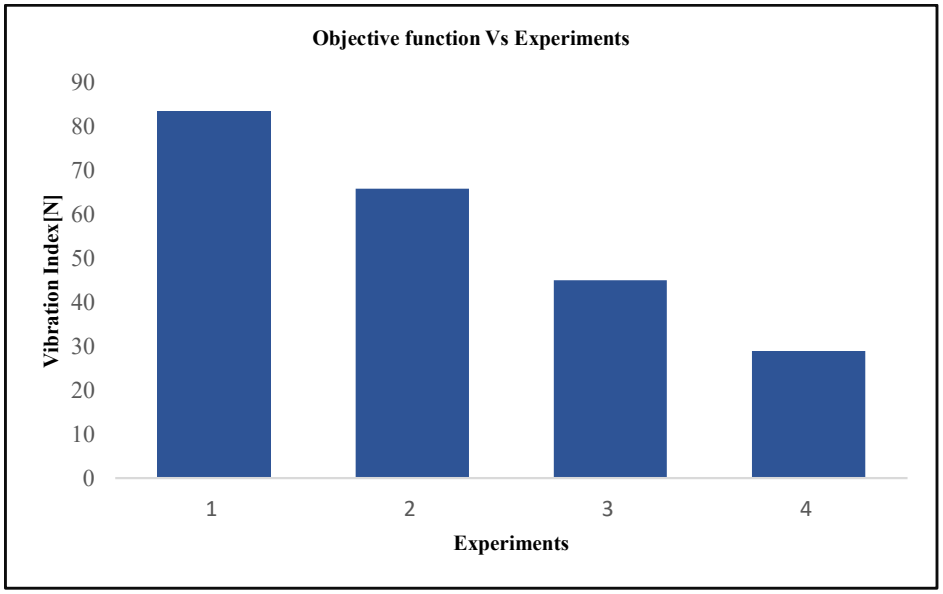

Figure 40. Comparison of the vibration index for the baseline vs optimization cases

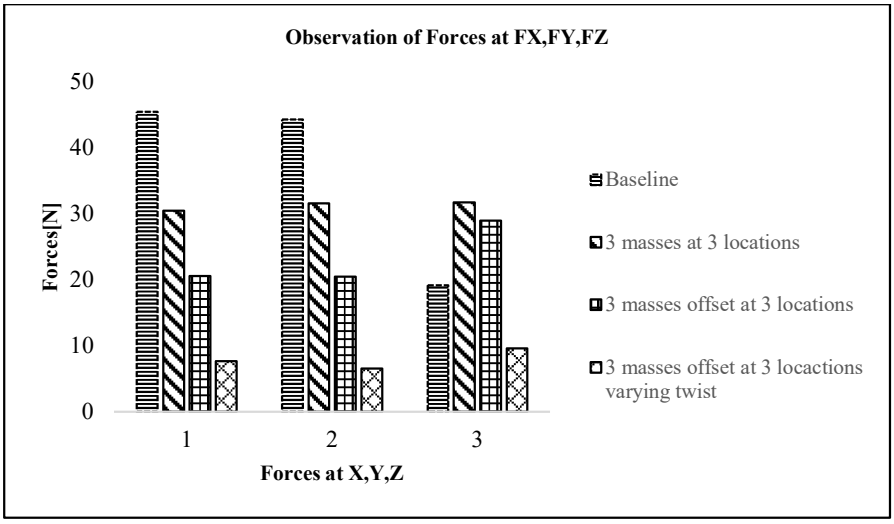

Figure 41. Comparison of the hub 4/rev force components for baseline and optimization iterations

Along with the objective function, the forces and moments components along the three dimensions of baseline vaules are compared with the best parameters achieved through optimization. The plots can be observed through Figure 41 and Figure 42.

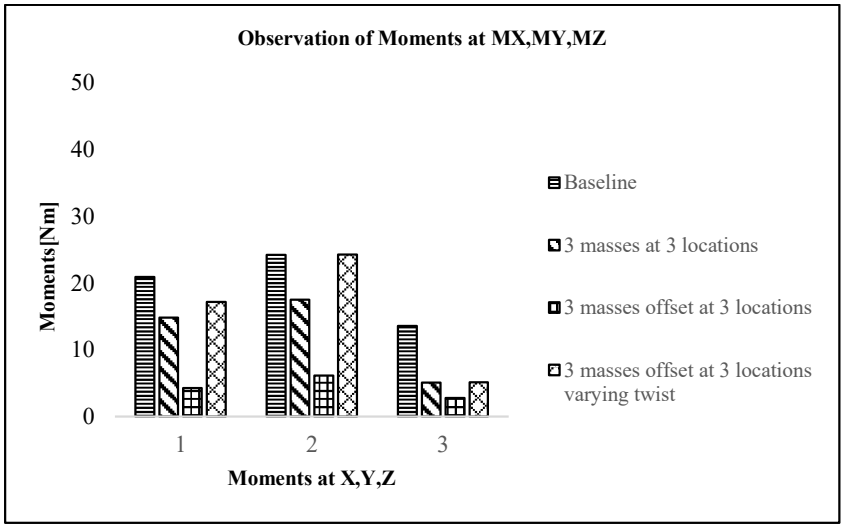

Figure 42. Comparison of the hub 4/rev moment components for baseline and optimization iterations

7. Campbell diagrams and mode shapes

In general, in the design of rotors, the natural frequencies of the blades are to be placed away from the integral multiples of the design rotor speed frequencies. Coincidence or near-coincidence of the blade natural frequencies with the multiples of rotor frequencies results in resonance conditions. The farther the blade natural frequencies are from these values, the vibratory loads also are reduced. Figures 43-45 compare the Campbell diagram of the helicopter baseline rotor blade with those of the three optimized rotors. The frequencies of interest are the second flap, second lag and the first torsion modes.

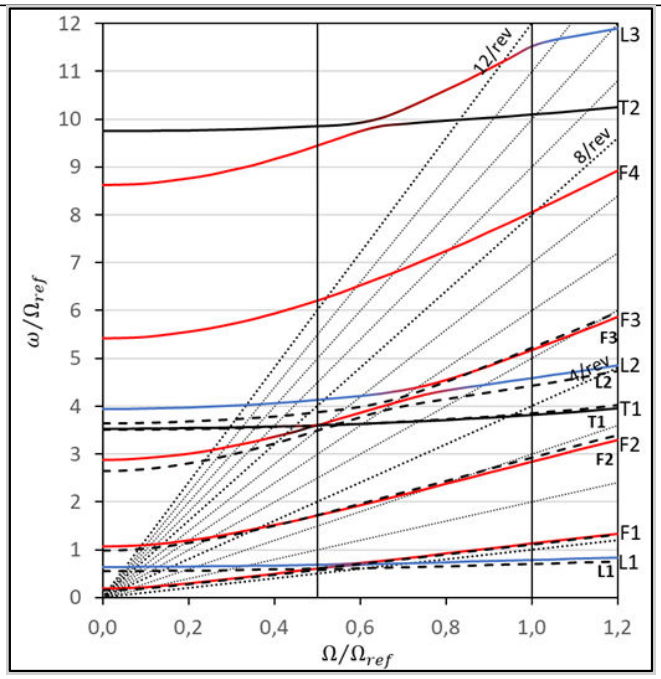

Figure 43. Campbell diagram for case I juxtaposed with first six frequencies of the baseline blade

In Figure 43, it is seen that the second flap frequency for case I (3 masses with no offsets) is placed farther away from the 3/rev than that for the baseline case. For case II (3 masses with elastic axis offset), as seen in Figure 44, the second flap frequency is even further away from the resonance frequency. This could partly explain the reduction in vibration index from the baseline to case I to case II. The 4/rev pitch and roll moments in the fixed hub frame are affected by the 3/rev flapwise moment. For case III (case II + additional geometric twist), as seen in Figure 45, the second flap frequency hasn't changed much from that of case II indicating less influence of the additional geometric twist on this frequency.

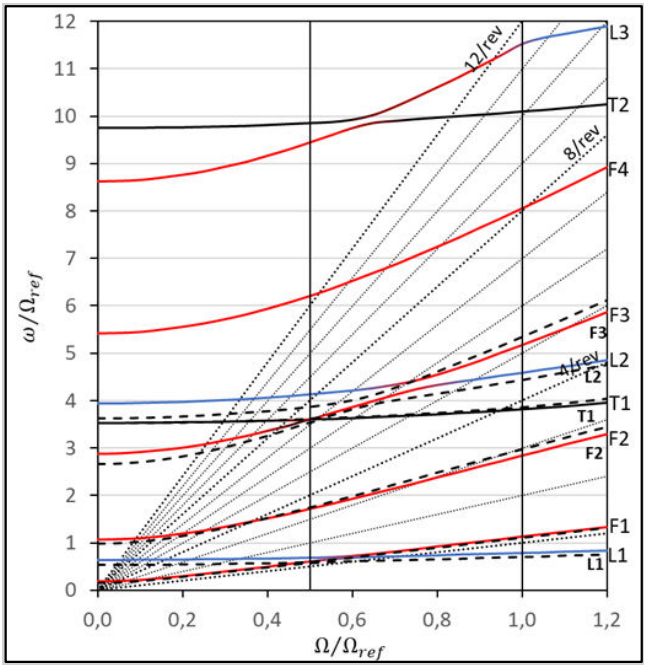

Figure 44. Campbell diagram for case II juxtaposed with first six frequencies of the baseline blade

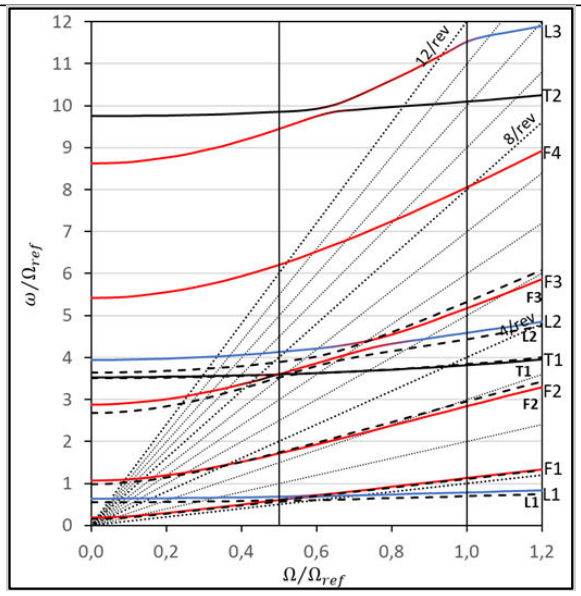

Figure 45. Campbell diagram for case III juxtaposed with first six frequencies of the baseline blade

Another contribution to the change in the hub vibratory loads can be observed from the mode shape diagrams. Mode shape changes result in change of the generalized forces on the rotor beam and this also influences the hub loads. Generalized forces depend on the forcing aerodynamic loading also, however this will not be examined in the current work. Figure 46 shows the mode shapes of the second flap frequency for the baseline blade and those of cases I and II. It is seen that there is a clear change in the shape as well as a shift in the node location from the baseline to cases I and II. The difference in the mode shapes between cases I and II are highlighted in Figure 47. It is to be noted that the root flap bending moment of the blade translates to the pitch and roll moments in the hub-fixed coordinate system. The 4/rev pitch and roll moments get contributions from 3/rev flap bending moments.

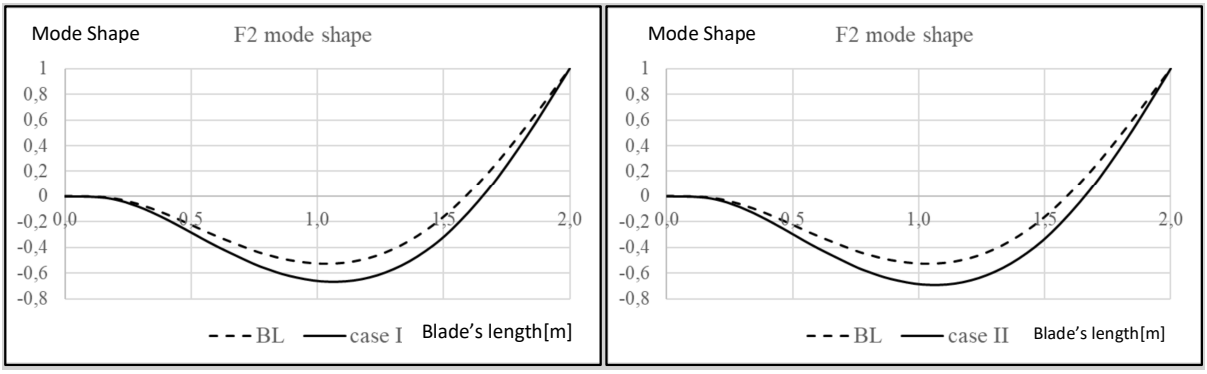

Figure 46. Mode shapes of the second flap frequency for the baseline blade vs case I & case II

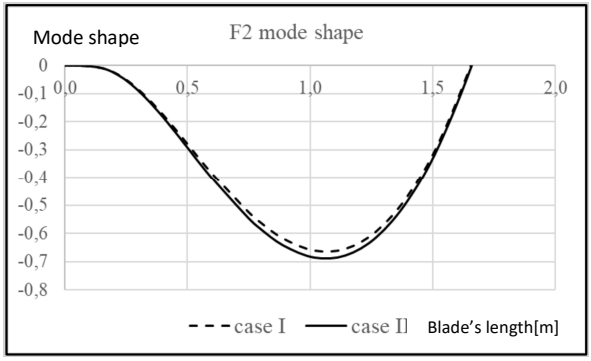

Figure 47. Comparing the mode shapes of the second flap frequencies for case I & case II

8. Conclusion

The goal of the current work was to obtain a rotor blade configuration which has less hub vibratory loads than the baseline HART II blade using passive techniques like addition of non-structural lumped masses along spanwise and chordwise locations. For this purpose, an optimization procedure was developed which involves integrating VAST (Versatile Aerodynamic Simulation Tool) into the workflow integrated environment RCE (Remote Control Environment) using Single-Objective Genetic optimization algorithm.

Initially to test the optimizer and process of optimization and integration of tools in RCE, an experiment is carried out by integrating Fusion 360 and FreeCAD. The main objective is to retain minimal material which is sufficient to withstand the stresses of the rectangular steel plate with a circular hole. The component is designed through Fusion 360 gets exported to FreeCAD for the Finite Element Analysis. The design variables for the optimization process are diameter of the circular hole, the distance between the center of the co-ordinate system and the center of hole towards X direction and the distance between the center of the coordinate system and the center of hole towards Z direction. To achieve the best parameters and best design variables for the optimization process both Single Objective Genetic Algorithm and Evolutionary Algorithm were implemented. The best parameters and best objective function are achieved through Single Objective Algorithm compared to the parameters obtained through Evolutionary algorithm. This boosted up the confidence to implement the optimization process using baseline HART II blade through passive methods in RCE.

A sensitivity analysis was first carried out which indicated that a lumped mass which was placed near the tip region and aft of the elastic axis reduces the vibration index the most. Subsequent optimization case with three lumped masses also gave a similar result with the vibration index reduced by almost 50%. Among the individual hub load 4/rev components, except for the vertical shear, all of them showed a reduction in values from those of the baseline case.

8.1. Recommendations for future scope

This thesis included the reduction of vibration to helicopter rotor blades applying passive method by placing tuning masses based on Single objective genetic algorithm in a workflow-integrated environment RCE. This procedure can also be used for increased performance by increasing more design variables and also implementing for other flight conditions.

As all the analysis can be done with RCE, the improved models can lead to more accurate results and will be user-friendly if, RCE itself can trigger the tool and terminates after its execution, so batch files are not required to integrate and execute tools, the optimization process time in providing the best parameters and best objective function is less and more accurate. Finding the error messages and inability to functioning of convergence are the main drawbacks of Optimizer in RCE. Hence, RCE's optimizer can be updated with more recent techniques.

9. References

1. Johnson, W., "Helicopter Theory," Dover Publications, Inc., 1994
2. Watkinson, J., "The Art of the Helicopter," Elsevier, 2004
3. Bielawa, R.L., "Rotary Wing Structural Dynamics and Aeroelasticity," AIAA Education Series, 2005
4. Leishmann J.G., "Principles of Helicopter Aerodynamics," Cambridge Aerospace Series, 2006
5. Plamen Antonov's Pages/Photography/Themes/Get Close!/Aircraft from Close By (pantonov.com)
6. Hodges D.H., "Aeromechanical Stability of Helicopters with a Bearingless Main Rotor – Part 1: Equations of Motion," NASA Technical Memorandum No. 78459, 1978,
7. Arnold, L., "Aerodynamics of the Helicoper," Frederick Ungar Publishing Co., 1985
8. Bramwell, A.R.S., Done, G., Balmford, D., "Bramwell's Helicopter Dynamics," Butterworth-Heinemann, 2001
9. Brentner, K.S., Farassat, F., "Modeling Aerodynamically Generated Sound of Helicopter Rotors," Progress in Aerospace Sciences, Vol.39, 2003, pp.83-120
10. Veca, A.C., "Vibration Effects on Helicopter Reliability and Maintainability," USAAMRDL Technical Report No.73-11, 1973
11. "Helicopter Fatigue Design Guide," General Editor F.P. Liard, AGARDograph No.292, 1983
12. Mansfield N.J., "Human Response to Vibration," CRC Press LLC, 2005, pp.14-16
13. Harrer, K., Yniguez, D., Majar, M., Ellenbecker, D., Estrada, N., Geiger, M., "Whole Body Vibration Exposure for MH-60S Pilots," 43th SAFE Association Symposium, Utah, 2005
14. Auffret, R., Delahaye, R.P., Metges, P.J., Vicens, "Vertebral Pain in Helicopter Pilots," NASA Technical Memorandum No.75792, 1978
15. Straub, F.K., Byrns, E.V., "Application of Higher Harmonic Blade Feathering on the OH-6A Helicopter for Vibration Reduction," NASA Contractor Report, 1986
16. Inman, D.J., "Vibration with Control," John Wiley and Sons Ltd, 2006, pp.145-148
17. Pierce, G.A., Hamouda M.N.H., "Helicopter Vibration Suppression Using Simple Pendulum Absorbers on the Rotor Blade", NASA Contractor Report, 1982
18. Nguyen, K.Q., "Higher Harmonic Control Analysis for Vibration Reduction of Helicopter Systems," NASA Technical Memorandum No.103855, 1994, pp.2-11
19. Jacklin, S.A., Haber, A, Simone, G., Norman, T.R., Kitaplioglu C., Shinoda, P., "Full-Scale Wind Tunnel Test of an Individual Blade Control System for a UH-60 Helicopter,", American Helicopter Society, 2002
20. Millott, T.A., Friedmann, P.P., "Vibration Reduction in Helicopter Rotors Using an Actively Controlled Partial Span Trailing Edge Flap Located on the Blade," NASA Contractor Report No. 4611, 1994
21. "Smart Structures Technology: Innovations and Applications to Rotorcraft Systems," General Editor I. Chopra, University of-Maryland Collage Park, Maryland, 1997, pp.8-9
22. Doman, G.S., "Research Requirements for the Reduction of Helicopter Vibration," NASA Contractor Report No.145116, 1976
23. Ko, T.W.H., "Design of Helicopter Rotor Blades for Optimum Dynamic Characteristics", PhD Dissertation, Washington University Sever Institute of Technology, Washington, 1984
24. Friedmann, P.P., Celi, R. "Structural Optimization of Rotor Blades with Straight and Swept Tips Subject to Aeroelastic Constraints", Recent Advances in Multidisciplinary Analysis and Optimization, NASA Conference Publication, Part1, 1989, pp.145-162
25. Peters, D.A., Cheng Y.P., "Optimization of Rotor Blades for Combined Structural, Performance, and Aeroelastic Characteristics", Recent Advances in Multidisciplinary Analysis and Optimization, NASA Conference Publication, Part1, 1989, pp.163-180
26. Lee, J., Hajela, P., "Parallel Genetic Algorithm Implmentation in Multidisciplinary Rotor Blade Design," AHS Technical Specialists' Meeting on Rotorcraft Structures, Williamsburg, 1995
27. Ganguli, R., "Optimum Design of a Helicopter Rotor for Low Vibration Using Aeroelastic Analysis and Response Surface Methods," Journal of Sound and Vibration Vol. 258, Issue 2,2002, pp,327-344
28. Bhadra, S., Ganguli, R., "Aeroelastic Optimization of a Helicopter Rotor Using Orthogonal Array Based Metamodels," AIAA Journal Vol. 44 No. 9, 2006, pp.1941-1951
29. Murugan, S., Ganguli, R., Harursampath, D., "Robust Aeroelastic Optimization of Composite Helicopter Rotor," International Conference on Engineering Optimization, Rio De Janerio, 2008

30. Glaz, B., Geol, T., Liu, L., Friedmann, P.P., Haftka, R. T., "Multiple-Surrogate Approach to Helicopter Rotor Blade Vibration Reduction," AIAA Journal Vol. 47 No. 1, 2009, pp.271-282
31. Viswamurthy, S.R., Ganguli, R., "An Optimization Approach to Vibration Reduction in Helicopter Rotors with Multiple Active Trailing Edge Flaps," Aerospace Science and Technology Vol. 8 Issue 3,2004, pp.185-194
32. Kvaternik, R.G., Murthy, T.S., "Airframe Structural Dynamic Considerations in Rotor Design Optimization," NASA Aeroelasticity Handbook Vol.2 Part 2,pp.13.1-13.3
33. Harrison R., Hansford, B., "BERP IV The Design Development and Testing of an Advanced Rotor Blade", AHS 64th Forum, Montreal, 2008
34. Houbolt, J.C., Brooks, G., "Differential Equations of Motion for Combined Flapwise Bending, Chordwise Bending, And Torsion of Twisted Non-Uniform Rotor Blades," NACA Technical Note No. 3905, 1957
35. Johnson, W., "Airloads, Wakes, and Aeroelasticity," NASA Contractor Report No. 177551, 1990
36. Seddon, J., "Basic Helicopter Aerodynamics," BSP Professional Books, 1990
37. Padfield, G.D., "Helicopter Flight Dynamics," Blackwell Publishing, 2007
38. Cugnon, F., Eberhard, A., "Aeroelastic Modeling of the Hub and Blade Rotor System of the Nicetrip Tilt-Rotor Aircraft Using Finite Element Multibody Approach," Multibody Dynamics 2011 ECCOMAS Thematic Conference, Brussels, 2011
39. Pritchard,J.I, Adelman M.H , "Optimizing Tuning Masses for Helicopter Rotor Blade Vibration Reduction including Computed Air loads and Comparison with Test Data", NASA Technical Memorandum, AVSCOM Technical Report, January 1992
40. DLR- Institute for Software Technology, "User Guide For RCE", Köln, Germany
41. DLR- Institute for Software Technology, "User Guide for VAST", Köln, Germany